R. A. Lohnes, T. J. Wipf, F. W. Klaiber,
B. E. Conard, K. W. Ng

Investigation of Plastic Pipes for Highway Applications: Phase II

November 1997

Sponsored by the
Project Development Division of the
Iowa Department of Transportation and the
Iowa Highway Research Board

Iowa DOT Project HR-373A

Iowa Department of Transportation

Final

REPORT

IOWA STATE UNIVERSITY
OF SCIENCE AND TECHNOLOGY

Department of Civil and Construction Engineering

The opinions, findings, and conclusions expressed in this publication are those of the authors and not necessarily those of the Project Development Division of the Iowa Department of Transportation or the Iowa Highway Research Board.

R. A. Lohnes, T. J. Wipf, F. W. Klaiber,
B. E. Conard, K. W. Ng

Investigation of Plastic Pipes for Highway Applications: Phase II

Sponsored by the
Project Development Division of the
Iowa Department of Transportation and the
Iowa Highway Research Board

Iowa DOT Project HR-373A

Final

REPORT

IOWA STATE UNIVERSITY
OF SCIENCE AND TECHNOLOGY

Iowa Department of Transportation

Department of Civil and Construction Engineering

Abstract

It is generally accepted that high density polyethylene pipe (HDPE) performs well under live loads with shallow cover, provided the backfill is well compacted. Although industry standards require carefully compacted backfill, poor inspection and/or faulty construction may result in soils that provide inadequate restraint at the springlines of the pipes thereby causing failure. The objectives of this study were: 1) to experimentally define a lower limit of compaction under which the pipes perform satisfactorily, 2) to quantify the increase in soil support as compaction effort increases, 3) to evaluate pipe response for loads applied near the ends of the buried pipes, 4) to determine minimum depths of cover for a variety of pipes and soil conditions by analytically expanding the experimental results through the use of the finite element program CANDE.

The test procedures used here are conservative especially for low-density fills loaded to high contact stresses. The failures observed in these tests were the combined effect of soil bearing capacity at the soil surface and localized wall bending of the pipes. Under a pavement system, the pipes' performance would be expected to be considerably better. With those caveats, the following conclusions are drawn from this study.

Glacial till compacted to 50% and 80% provides insufficient support; pipe failure occurs at surface contact stresses lower than those induced by highway trucks. On the other hand, sand backfill compacted to more than 110 pcf (17.3 kN/m^3) is satisfactory. The failure mode for all pipes with all backfills is localized wall bending.

At moderate tire pressures, i.e. contact stresses, deflections are reduced significantly when backfill density is increased from about 50 pcf (7.9 kN/m^3) to 90 pcf (14.1 kN/m^3). Above that unit weight, little improvement in the soil-pipe system is observed.

Although pipe stiffness may vary as much as 16%, analyses show that backfill density is more important than pipe stiffness in controlling both deflections at low pipe stresses and at the ultimate capacity of the soil-pipe system. The rate of increase in ultimate strength of the system increases nearly linearly with increasing backfill density.

When loads equivalent to moderate tire pressures are applied near the ends of the pipes, pipe deflections are slighly higher than when loaded at the center. Except for low density glacial till, the deflections near the ends are not excessive and the pipes perform satisfactorily. For contact stresses near the upper limit of truck tire pressures and when loaded near the end, pipes fail with localized wall bending.

For flowable fill backfill, the ultimate capacity of the pipes is nearly doubled and at the upper limit of highway truck tire pressures, deflections are negligible.

All pipe specimens tested at ambient laboratory room temperatures satisfied AASHTO minimum pipe stiffness requirements at 5% deflection. However, nearly all specimens tested at elevated pipe surface temperatures, approximately 122°F (50°C), failed to meet these requirements. Some HDPE pipe installations may not meet AASHTO minimum pipe stiffness requirements when installed in the summer months (i.e. if pipe surface temperatures are allowed to attain temperatures similar to those tested here). Heating of any portion of the pipe circumference reduced the load carrying capacity of specimens.

The minimum soil cover depths, determined from the CANDE analysis, are controlled by the 5% deflection criterion. The minimum soil cover height is 12 in. (305 mm). Pipes with the poor silt and clay backfills with less than 85% compaction require a minimum soil cover height of 24 in. (610 mm). For the sand at 80% compaction, the A36 HDPE pipe with the lowest moment of inertia requires a minimum of 24 in. (610 mm) soil cover. The C48 HDPE pipe with the largest moment of inertia and all other pipes require a 12 in. (305 mm) minimum soil cover.

Table of Contents

Page

List of Figures vii

List of Tables ix

1. **INTRODUCTION** 1

2. **EXPERIMENTAL TEST PROGRAM** 3
   - 2.1 Pipe Characteristics 3
   - 2.2 Backfill Characteristics 4
   - 2.3 Test Equipment and Procedures 5

3. **EXPERIMENTAL TEST RESULTS** 9
   - 3.1 Pipe Response During Backfilling 9
   - 3.2 Pipe Response under Service and Failure Loads 9
   - 3.3 Influence of Soil Characteristics on Pipe Capacity 13
   - 3.4 Pipe Depending on Backfill Envelope 16
   - 3.5 Pipe Backfill Response and Highway Loads 17
   - 3.6 Influence of Pipe Characteristics on Response to Surface Loads 19
   - 3.7 Pipe Response under Loads Applied near the Pipe Ends 20
   - 3.8 Ultimate Capacity of Pipe-Soil System 24
   - 3.9 Effect of Temperature on HDPE Pipe Strength 26
     - 3.9.1 Parallel Plate Testing 27
     - 3.9.2 Pipe Stiffness Results 29

4. **NUMERICAL ANALYSIS USING Culvert ANalysis and DEsign (CANDE)** 35
   - 4.1 General Background 35
   - 4.2 Objective and Scope 38
   - 4.3 Validation of Methodology 39
   - 4.4 Comparison of Analysis with Experimental Data 43
   - 4.5 Mesh Sensitivity Under Surface Loads 51
   - 4.6 Analytical Minimum Soil Cover 52

5. **CONCLUSIONS** 61

6. **RECOMMENDED RESEARCH** 63

7. **ACKNOWLEDGEMENTS** 65

8. **REFERENCES** 67

List of Figures

Page

Figure 1. In-situ test frame 7

Figure 2. Changes in Section 4 vertical diameters during installation and failure loading. 10

Figure 3. Soil penetration by the loaded "footprint" 12

Figure 4. Localized bending failure of the pipe specimen beneath the loaded "footprint". 12

Figure 5. Changes in Section 4 horizontal diameters during installation and failure loading 14

Figure 6. Percent net vertical deflection at Section 4 during failure loading 15

Figure 7. Increase in ultimate load carrying capacity versus the average dry density of the overburden soil at Section 4 16

Figure 8. Changes in vertical pipe diameters as a function of backfill depth 18

Figure 9. Ultimate capacity and ultimate contact stress of each pipe-soil system 19

Figure 10. Net vertical diameter changes at an applied stress of 7,000 psf 21

Figure 11. Net vertical diameter changes at an applied stress of 7,000 psf normalized by the pipe stiffness factor, EI 21

Figure 12. Percent pipe deflection during field test service loading 22

Figure 13. Percent pipe deflection during failure loading field tests 25

Figure 14. Details of instrumentation and location of heat lamps used in parallel plate tests 28

Figure 15. Load versus changes in pipe diameter: Specimen A48 32

Figure 16. Load versus circumferential strain: Specimen A48 33

Figure 17. Key for strains presented in Figure 16 34

Figure 18. The schematic model of solution level 1 36

Figure 19. The schematic trench model of solution level 2 37

Page

Figure 20. Loading conditions of a strip load, q, and a concentrated load, Q 40

Figure 21. Schematic diagram of the finite element mesh of a 24 in. pipe for Comparison with Katona (1990) 42

Figure 22. Comparison between Katona's and author's analytical data 43

Figure 23. Schematic diagram of the typical finite element mesh of the 36 in. pipe used for comparison with field test data 45

Figure 24. The finite element model of field test ISU4 (mesh shown in Figure 23) 46

Figure 25. The finite element model of field test ISU8 (mesh shown in Figure 23) 47

Figure 26. The finite element model of field test ISU9 (mesh shown in Figure 23) 48

Figure 27. Comparison of ISU4 experimental data with analytical data 50

Figure 28. Comparison of ISU8 experimental data with analytical data 50

Figure 29. Comparison of ISU9 experimental data with analytical data 51

Figure 30. Schematic diagram of the modified finite element mesh of the 36 in. pipe 54

Figure 31. Comparison of the analytical data of the CANDE models for meshes Shown in Figures 23 and 30 55

Figure 32. CANDE vertical deflection predictions for 36 in. pipe from Manufacturer A 56

Figure 33. CANDE vertical deflection predictions for 36 in. pipe from Manufacturer C 56

Figure 34. CANDE vertical deflection predictions for 48 in. pipe from Manufacturer A 57

Figure 35. CANDE vertical deflection predictions for 48 in. pipe from Manufacturer C 57

List of Tables

Page

Table 1. HDPE pipe properties 3

Table 2. Summary of pipes tested and backfill materials 6

Table 3. Estimated bearing capacity of soil cover 11

Table 4. Pipe deflections at 10,000 psf (479 kPa) contact surface pressure 24

Table 5. Pipe deflections at ultimate capacity 26

Table 6. Properties of parallel plate specimens tested 28

Table 7. Pipe stiffnesses at ambient and elevated temperatures determined using ASTM D2412 30

Table 8. Polyethylene material properties of 24 in. (610 mm) HDPE pipes used by Katona (1990) 41

Table 9. Duncan model parameters of SC85 and SC100 41

Table 10. Manufacturer's polyethylene material properties of 36 in. (915 mm) And 48 in. (1,220 mm) HDPE pipes which were field tested 44

Table 11. Duncan soil parameters of the surrounding soil of the field test Specimen (as per CANDE) 49

Table 12. Duncan soil parameters of SW80, SW95, and CL45 53

Table 13. Minimum soil cover height in inches 59

1. INTRODUCTION

This report summarizes the findings of Iowa Department of Transportation (Iowa DOT) project HR-373A, "Investigation of Plastic Pipes for Highway Applications, Phase II". For additional details on this project, see the theses of Conard *(1997)* and Ng *(1997)*. The results of the Phase I of this investigation are in the final report to HR-373 (Klaiber et al, *1996*).

It is generally accepted that corrugated polyethylene pipe performs well under live loads with shallow cover, provided that the backfill is well compacted. Watkins et al *(1983)* conducted experimental studies of 24 in. (610 mm) diameter pipe under AASHTO H-20 standard truck loads to develop recommendations for minimum cover depths. The soils studied in these tests included a mixture of sandy clay silt and sandy silty clay compacted between 80% and 95% standard density which classified as CL and an uncompacted gravel. Katona et al *(1990)* applied the finite element program CANDE to evaluate a number of pipe and soil characteristics under a variety of surface loads. The soil data that Katona used included 85% and 100% compacted silty clayey sand SC with pipe diameters ranging from 12 in. (305 mm) to 36 in. (914 mm).

Although industry standards require carefully compacted backfill, concern exists that poor inspection and/or faulty construction may result in soils that provide inadequate passive restraint at the springlines of the pipes thereby leading to failure. One objective of this study was to determine the response of the pipes under poor bedding and backfill conditions and to define a lower limit of compaction under which the pipes would perform satisfactorily. A second objective was to quantify the increase in soil support as compaction effort increased. A third objective of this investigation was to evaluate pipe response for loads applied near the ends of the buried pipes. Finally, the general software CANDE was used to analytically determine minimum acceptable depths of cover for a variety of pipes and soil conditions.

2. EXPERIMENTAL TEST PROGRAM

2.1. Pipe Characteristics

High density polyethylene pipes, 20 ft (6.1 m) long from two different manufacturers, identified as A and C, were tested with various backfills. These pipes, 36 in. (915 mm) and 48 in. (1,220 mm) in diameter from Manufacturer A and the 48 in. (1,220 mm) diameter pipe from Manufacturer C were evaluated in parallel plate tests. Table 1 presents data on wall thickness, stiffness, and the EI as calculated by ASTM D2412, for all three pipes. These pipes are designated A36, C36, and C48 respectively, indicating the manufacturer and pipe diameter in inches.

Table 1. HDPE pipe properties.

Pipe Type/diameter in. (mm)	Wall thickness in. (mm)	ASTM Stiffness Psi (kPa)	EI lb-inch (MPa-mm)
A36 (915)	0.30 (7.60)	29.99 (210)	26,030 (2,940)
A48 (1,220)	0.28 (7.10)	20.62 (140)	42,430 (4,795)
C48 (1,220)	0.18 (4.60) inner wall	22.46 (155)	46,190 (5,220)

In addition to the parallel plate tests, short specimens of the pipes (lengths equal to their inside diameter) were tested with the same loading arrangement that was used in the backfill tests. For these tests, four different backfill configurations were investigated: no backfill with the specimen in the saddle, sand backfill to 50% of the outside pipe diameter, sand backfill to 70% of the outside pipe diameter, and sand backfill to the crown of the pipe. The tests without backfill gave baseline data against which the results from the various backfill tests were compared and provided insight into the behavior of the various pipes.

2.2. Backfill Characteristics

Eleven field tests (ISU1-ISU4 and ISU7-ISU13) were conducted with varying configurations of backfill consisting of glacial till and granular material. Tests ISU1-ISU4 were completed in Phase I of this investigation (HR-373, 1996) and Tests ISU7-ISU13 were completed in this phase of the study. Tests ISU5 and ISU6, which were part of Phase II, were aborted because of instrumentation problems. The densities of the soils were measured with a nuclear density meter and with an Ely volumeter. The glacial till used in these tests classifies as CL-ML with a maximum standard proctor dry density of 118.1 pcf (18.6 kN/m^3). The granular material is classified as SW.

The bedding for all tests except ISU1 was Iowa DOT Class B with 15% of the pipe diameter in a saddle cut in the natural ground and a 2 in. (50.8 mm) layer of sand added. In these tests, the backfill was compacted in lifts that were 25% of the pipe diameters.

Tests ISU1 through ISU4 were conducted on 36 in. (915 mm) pipe from Manufacturer C and Tests ISU7 through ISU10 were conducted on 36 in. (915 mm) pipe from Manufacturer A. For Test ISU1, the glacial till was dumped into the excavation without compaction producing a highly variable backfill having unit weights ranging from 38 to 72 pcf (5.96 to 11.3 kN/m^3). The pipe was placed on the bottom of the trench without bedding.

The bottom of the excavation was 6 ft (1.8 m) wide and the sides were sloped 1 to 1. The bedding for all subsequent tests was Iowa DOT Class B with 15% of the pipe diameter in a saddle cut in the natural ground and a 2 in. (50.8 mm) layer of sand added. In these tests, the backfill was compacted in 9 in. (229 mm) lifts. This means that lifts 1 through 4 placed soil to the crown of the pipes and lifts 5 through 7 are the placement of soil above the tops of the pipes. The soil above the top of the pipe was 2 ft (0.61 m) deep and composed of compacted glacial till.

In Tests ISU2 and ISU4, compacted granular backfill was placed to 70% of the pipe diameter, i.e. 25.2 in. (640 mm). The remaining depth was filled with compacted till. In Test ISU3, the pipe was surrounded with an envelope of sand to a height of 1 ft (305 mm) above the top of the pipe; the remaining cover consisted of compacted glacial till.

In Tests ISU7 and ISU8, the backfill was glacial till compacted to about 80% and 95% standard proctor density, respectively, around pipe from Manufacturer A. In Test ISU9, the geometry of backfill placement was similar to that in Tests ISU2 and ISU4 but with pipe from Manufacturer A.

Tests ISU11 and ISU13 were conducted on 48 in. (1,220 mm) pipe from Manufacturer A, while Test ISU12 was conducted on 48 in. (1,220 mm) pipe from Manufacturer C. In Tests ISU10 and ISU13, 2 ft (610 mm) of flowable mortar (conforming to Iowa DOT Specification Sec. 2506) was poured on top of the sand which had been placed to 70% of the outside pipe diameter. After the flowable motor cured for 24 hours, crushed limestone (Iowa DOT Specification 4132) was placed to a height of 2 ft (610 mm) of overburden. Tests ISU9, ISU11, and ISU12 had 2 ft (610 mm) of compacted glacial till cover. The test conditions and average densities of the soils in each test are summarized in Table 2.

2.3. Test Equipment and Procedures

Detailed description of the test equipment and arrangement can be found in Phares *(1996)* and Klaiber et al *(1996)*. A brief description is provided here.

The loading system was designed to simulate surface live loads passing over the pipe with a concentrated load applied through a 12 in. (305 mm) square plate. Loads were applied by a hydraulic cylinder reacting against an overhead frame connected to concrete blocks weighing

Table 2. Summary of pipes tested and backfill materials.

Test Number	Pipe type and Diameter in inches	Side fill Material	Average Dry density pcf (kN/m^3)	Top fill Material	Average Dry density pcf (kN/m^3)
ISU1	C36	Till	55.8 (8.8)	Till	47.1 (7.4)
ISU2	C36	Sand	126.0 (19.8)	Till	116.3 (18.3)
ISU3	C36	Sand	125.9 (19.8)	Sand/Till	122.2 (19.2)
ISU4	C36	Sand	118.3 (18.6)	Till	127.7 (20.0)
ISU7	A36	Till	92.0 (14.4)	Till	93.3 (14.7)
ISU8	A36	Till	110.1 (17.3)	Till	111.7 (17.5)
ISU9	A36	Sand	96.1 (15.1)	Till	115.2 (18.1)
ISU10	A36	Sand	95.1 (14.9)	Flowable Mortar	N/A
ISU11	A48	Sand	93.6 (14.7)	Till	108.4 (17.0)
ISU12	C48	Sand	101.2 (15.9)	Till	112.9 (17.7)
ISU13	A48	Sand	N/A	Flowable Mortar	N/A

Approximately 80,000 lbs (355 kN). The loads were measured with a force transducer and applied at midlength of the pipe and at 5 ft (1.52 m) from each end of the pipes, i.e. three different load points. The test frame used is shown in Figure 1.

Horizontal and vertical deflections were measured with string type displacement potentiometers. Hoop and longitudinal strains were measured with electrical resistance strain gages at various sections along the pipes. Only deflection measurements are reported here as the trends

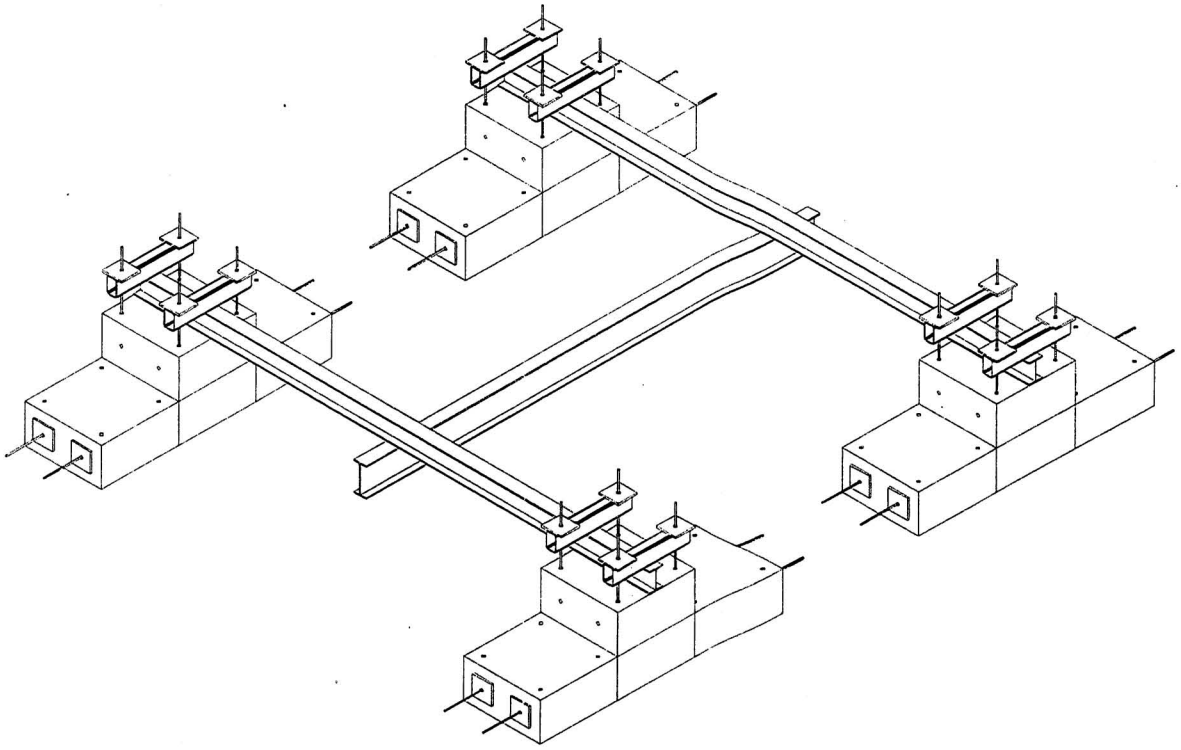

a. Schematic

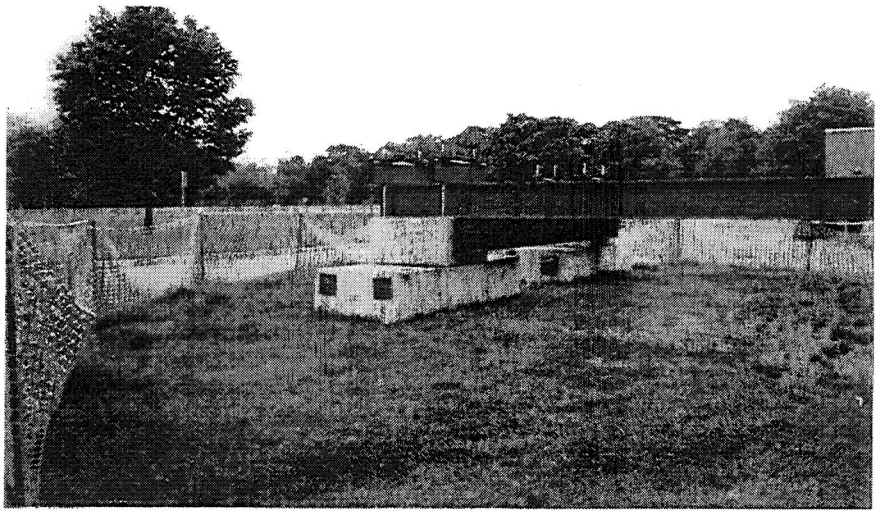

b. Photograph

Figure 1. In-situ test frame.

observed in the strain measurements are parallel to the trends observed with the deflection measurements.

The pipe deflections were measured during the backfilling and compaction process as well as during the application of the surface loads. The loads were applied directly to the soil surface without pavement layers. Service load tests were conducted applying contact stresses of 9,000 psf (431 kPa) to 14,400 psf (690 kPa) that would be expected from truck tire pressures. Upon completion of the service load tests, the pipes were loaded to failure at each of the three sections. Failure was defined by a decrease in load with increasing pipe deflections.

These tests provide a loading that is much more severe than would occur if a pavement were present. Elastic theory calculations indicate that for a soil cover of 2 ft (610 mm), the stresses at the top of the pipe are 10% of the contact stress. At contact stresses above the service range, for most tests, the load plate punched into the soil as the bearing capacity of overburden soil was exceeded. As one would expect, as the load plate moved closer to the pipe, the stresses in the pipe significantly increased.

3. EXPERIMENTAL TEST RESULTS

3.1. Pipe Response During Backfilling

Figure 2 shows the vertical deflections of the pipes during backfilling, surface loading, and failure loading. The numbers associated with each curve are the first seven tests previously described. Decreases in pipe diameter are designated as negative while expansions are positive. The left side of the graph shows deflection as a function of lift number and the right side of the graph shows deflections resulting from the surface loading where deflection is a function of contact stress.

In all tests, the vertical diameter increased during backfilling and the deflections ranged from about 0.2 to 1.7%. The horizontal deflections decreased accordingly to produce ovalization of the pipes during compaction. Pipes backfilled with the denser soils experienced greater deflections or more pronounced ovalization.

3.2. Pipe Response under Service and Failure Loads

For a typical AASHTO H truck, the contact stresses range from 65 psi to 100 psi (430 to 670 kPa) or 9,360 psf to 14,400 psf. Figure 2 shows that, for most tests in the load range of typical truck tire pressures, deflections are small. The exceptions are for the uncompacted till (Test ISU1) and the till compacted to 80% maximum density (Test ISU7). In these two cases failure occurs at contact stresses of about 8,000 psf (383 kPa) and 12,000 psf (575 kPa). These results are likely caused in part by the load plate punching into the soil.

Initially, the vertical diameter at the sections where load is applied gradually decreased. As the load is increased, the pipes return to their original diameter and the pipe walls reverse in curvature. After the stress-strain curves reach a maximum applied contact stress, the pipes exhibit

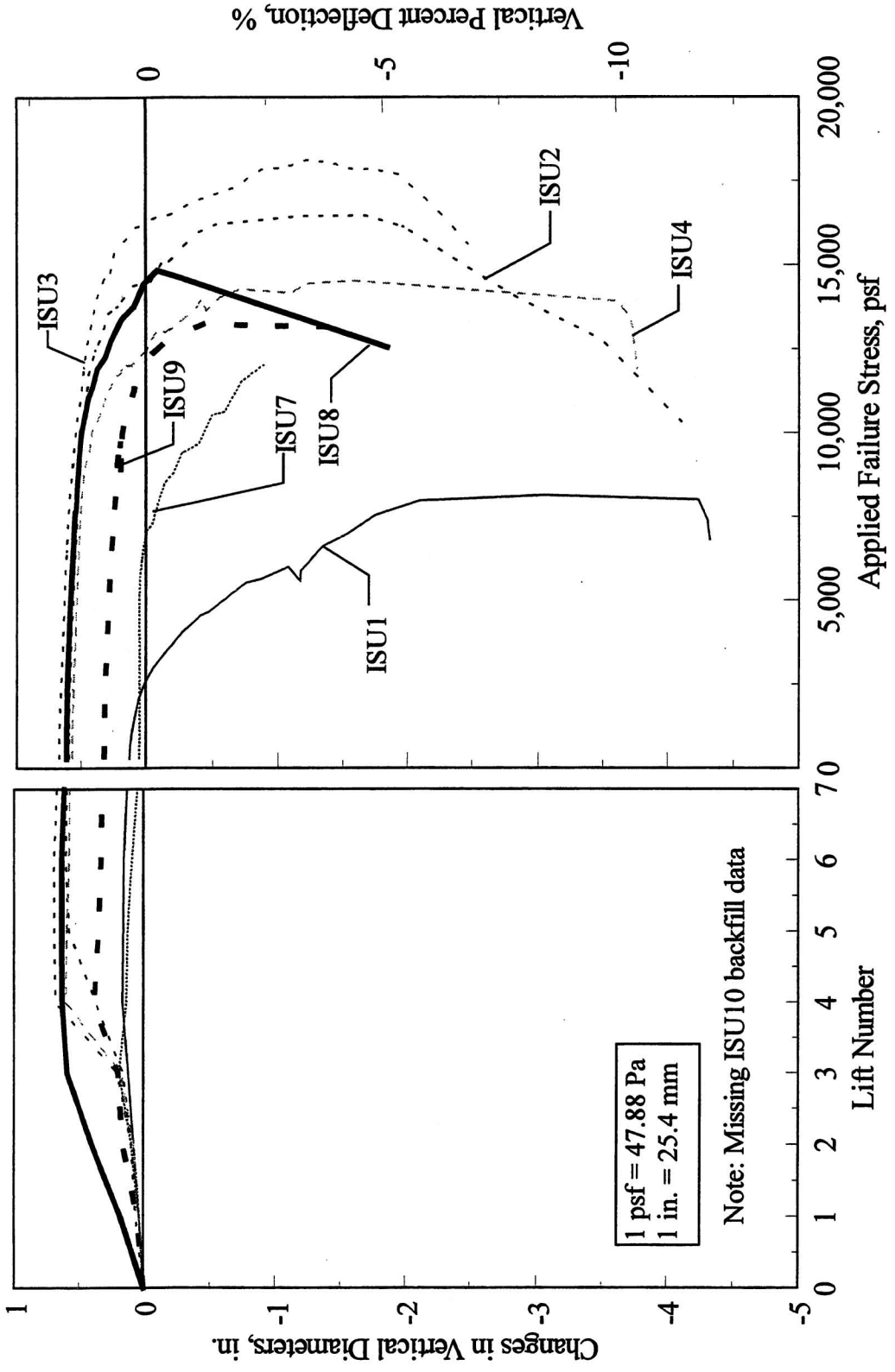

Figure 2. Changes in Section 4 vertical diameters during installation and failure loading.

strain-softening behavior with large reductions in vertical diameter and slight decreases in applied stress.

For all pipes, the failure initiated at vertical deflections smaller than 5% of the pipe diameter. This behavior is associated with the penetration of the loading plate into the soil and localized pipe wall bending. These two phenomena are shown in Figures 3 and 4, respectively.

The strain-softening phenomenon is likely exacerbated as a result of soil penetration. At the beginning of the loading process, the soil bearing capacity is larger than the contact stress, and the settlement of plate is small. Thus, without shearing or compressing the 24 in. (610 mm) soil cover, the vertical contact stress is distributed and transferred through soil cover to the crown of the pipe.

Estimates of bearing capacity of the soil cover, based on Meyerhof *(1963),* equations are shown in Table 3. The cohesions and friction angles used for calculating the theoretical bearing capacity are selected from CANDE-89 USER Manual (Musser, *1989*).

Table 3. Estimated bearing capacity of soil cover.

Field Test	Soil Friction Angle, Degree	Soil Cohesion, c Psi (Kpa)	Bearing Capacity psf (kPa)
ISU1	23	0 (0)	850 (41)
ISU2	15	2.8 (19.3)	6075 (127)
ISU3	15	2.8 (19.3)	6080 (127)
ISU4	15	5 (34.5)	2123 (102)
ISU7	19	5 (34.5)	2123 (102)
ISU8	15	9 (62)	6068 (291)
ISU9	15	9 (62)	6072 (291)

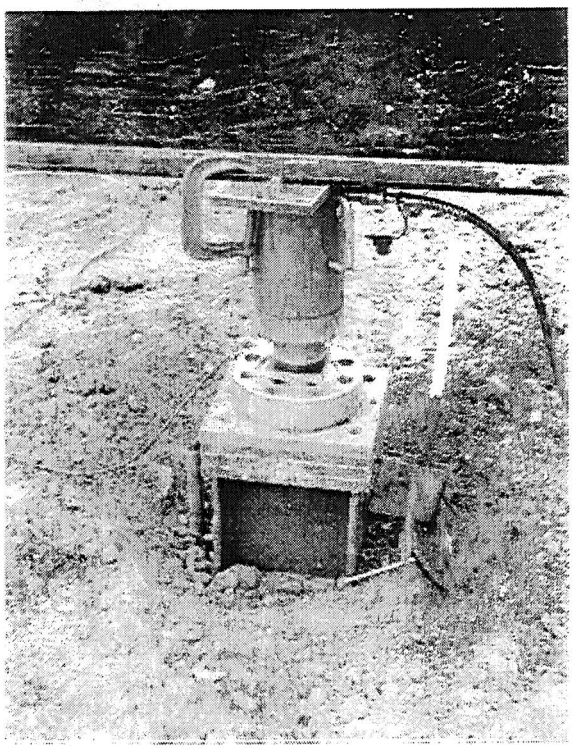

Figure 3. Soil penetration by the loaded "footprint".

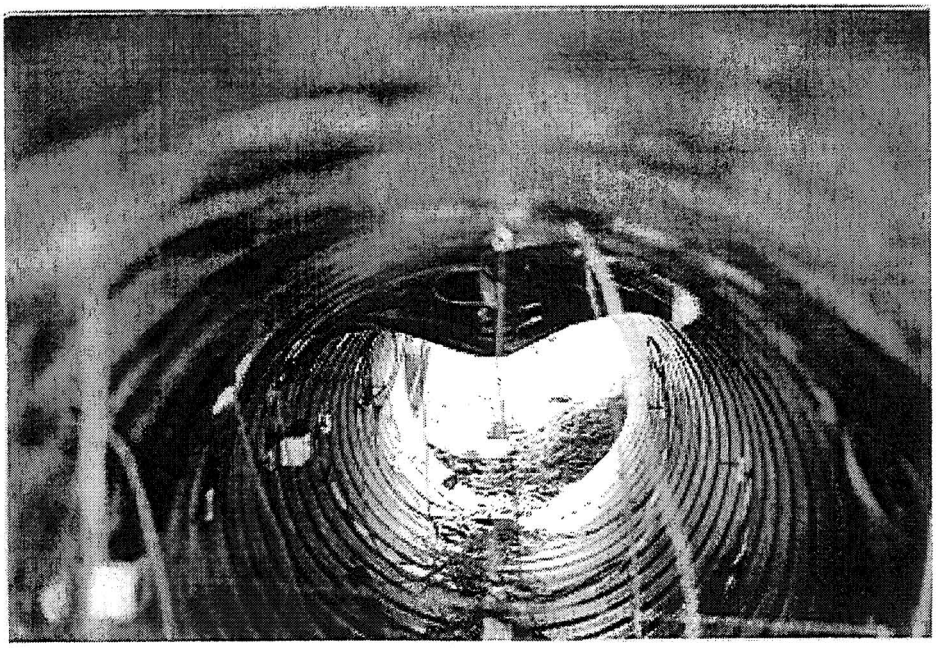

Figure 4. Localized bending failure of the pipe specimen beneath the loaded "footprint".

Comparing the bearing capacities shown in Table 3 with the load test data, the rate of change of pipe vertical deflection begins to increase after the contact stress exceeds the soil bearing capacity. For Tests ISU1 and ISU7, the vertical deflection rates start to increase at approximately 2,000 psf (96 kPa) and 4,000 psf (192 kPa), respectively. For the remaining tests, the vertical deflection rates begin to increase at approximately 11,000 psf (527 kPa). Generally, the applied contact stress at which the vertical deflection rate begins to increase is approximately twice the estimated bearing capacity. After exceeding the soil bearing capacity, the plate penetrates the soil cover and reduces the distance between the applied load and the crown of the pipe. Reduction of soil cover depth increases the vertical stress increment at the crown of the pipe; thus, the vertical deflection increases at a faster rate until it reaches the ultimate strength of the soil-pipe system. Continued reduction of soil cover leads to a stress increase at the crown of the pipe and eventual failure of the pipe.

Figure 5 shows the pipe horizontal deflections during the backfilling process and due to applied load on the pipe. For pipes with higher compacted backfill, with increasing contact stress the horizontal diameter remains smaller than the original diameter. In contrast, for pipe specimens with relatively lower compacted backfill such as in Tests 1 and 7, their horizontal diameters return to the original diameter and actually increase as applied loads increase. The magnitude of net horizontal deflection caused by the applied stress is relatively smaller than the net vertical deflection.

3.3. Influence of Soil Characteristics on Pipe Capacity

Figure 6 shows the net deflection of the pipes to failure as well as the net vertical deflection when loaded with the field test plate but without soil envelope backfill. Net deflection is deflection

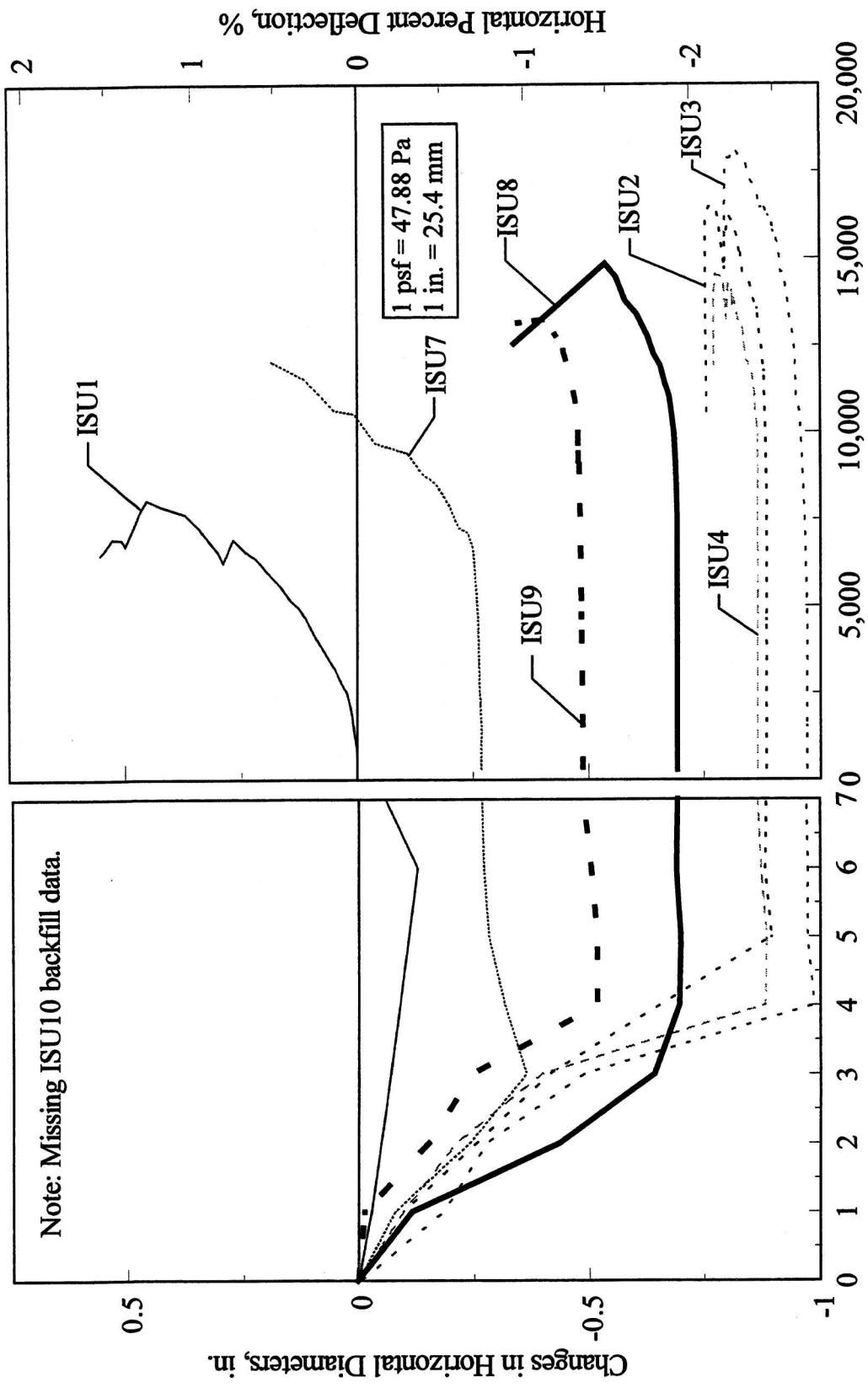

Figure 5. Changes in Section 4 horizontal diameters during installation and failure loading.

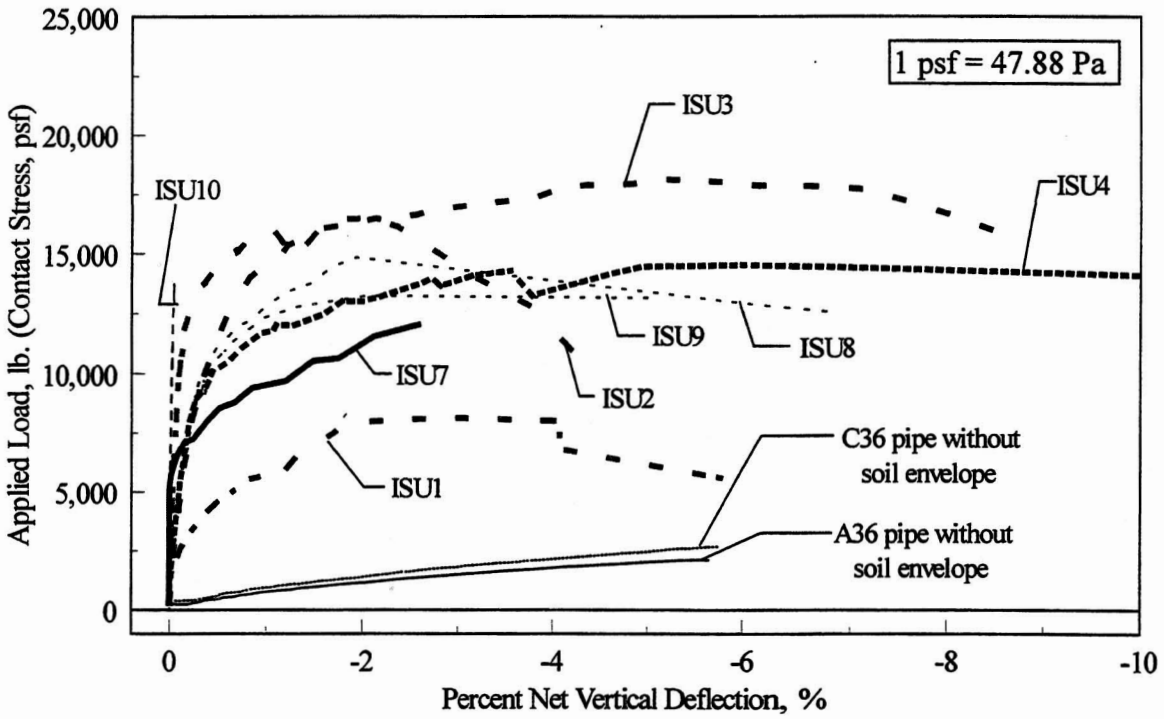

Figure 6. Percent net vertical deflection at Section 4 during failure loading.

due to applied surface loads and ignores initial ovalization of the pipes.

Referring to Figure 6, the ultimate capacity of each pipe-soil system occurs at approximately 2% vertical deflection. Also shown in Figure 6, the capacities of pipes A and C at 2% deflection are approximately 1,140 lb. (5.1 KN) and 1,390 lb. (6.2 KN), respectively. With a well compacted soil envelope around the pipe and a 2 ft (610 mm) soil cover, illustrated by Test 3, the ultimate capacity of the pipe is increased by approximately 16,615psf (13.9 kPa), or by a factor of 12. Even with poorly compacted till, shown in Test 1 the ultimate capacity is increased by approximately 6,600 lb (29.4 kN), or by a factor of 5.

The comparison of the gain in pipe structural capacity to soil quality is illustrated in Figure 7. The rate of increase in ultimate capacity by compacting the glacial till from 80% to 95% Standard Proctor is about three times greater than the rate by compacting it from 50% to 80% standard Proctor.

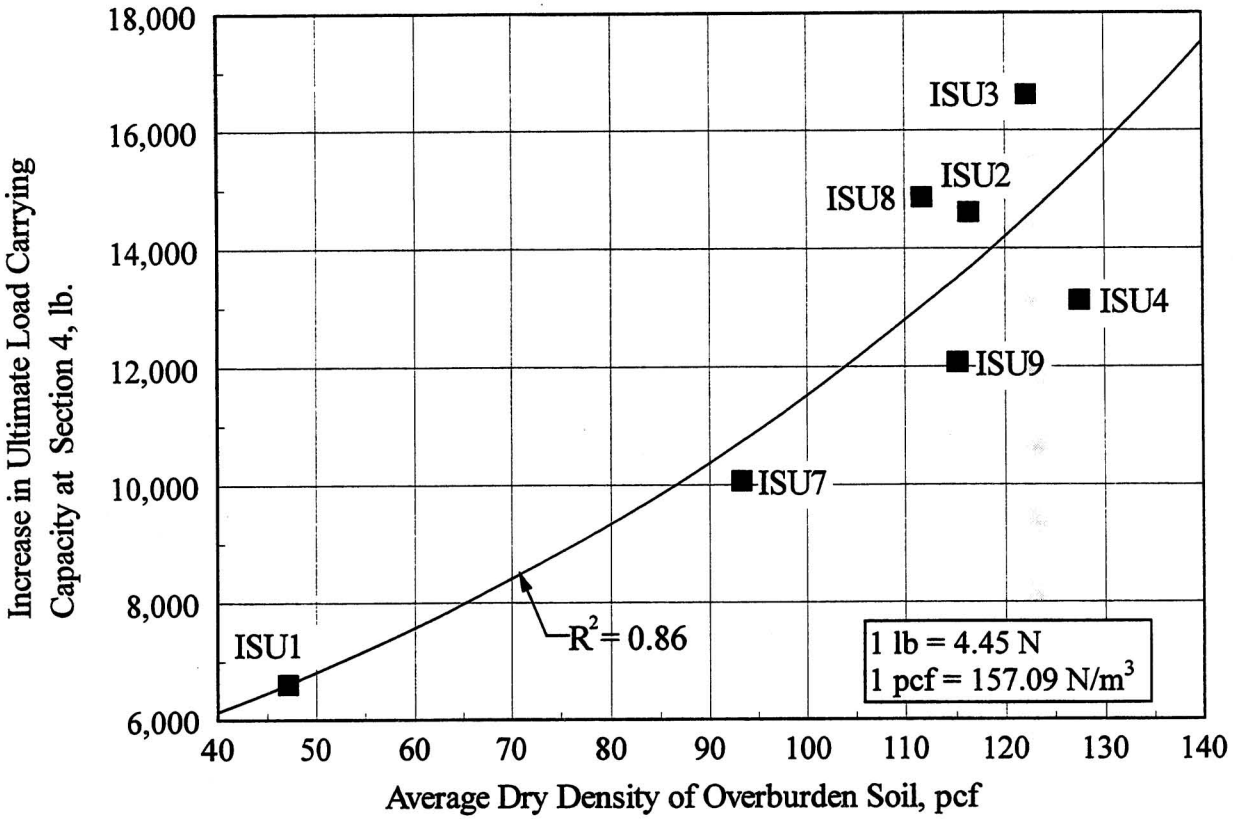

Figure 7. Increase in ultimate load carrying capacity versus the average dry density of the overburden soil at Section 4.

3.4. Pipe Dependence on Backfill Envelope

To establish the relative dependence of polyethylene pipes on backfill, four sets of tests were conducted on 36 in. (915 mm) and 48 in. (1,220 mm) pipes from Manufacturers A and C with the length of the pipes equal to the pipe diameter. For these tests, the load application system was identical to that used in the field tests on 20 ft (6.1 m) long pipes. In each set of tests, the pipes were subjected to loading with four backfill conditions: no backfill with pipes resting in the bedding saddle, sand backfill to the springline, sand backfill to 70% pipe diameter and sand backfill to the crown of the pipe. The testing arrangement in these field tests measured the local bending response of the pipe while the laboratory parallel plate tests measured the hoop strength of the pipe.

The changes in vertical pipe diameter in these four tests are shown in Figures 8a, 8b, 8c, and 8d, respectively. For the tests with no backfill, Figure 8a, the pipe response is nearly linear and all four pipes have load deflection curves that are similar. In Figure 8b where the backfill is at the springline, the pipes' responses become nonlinear and the loads to cause 5% deflection are nearly double the values observed in Figure 8a. As the backfill becomes higher in Figures 8c and 8d, the load deflection curves become increasingly convex upward and the pipes exhibit greater stiffness. This response reflects the effect of increasing restraint from the surrounding soil. In the backfill situations, the 48 in. (1,220 mm) pipe from Manufacturer C requires more load to produce the same deflection than the other 3 pipes. The difference between C48 and the other pipes suggests that this pipe is more highly dependent on backfill than the other three pipes because it gains stiffness more effectively than the other three pipes. This difference results from differences in pipe geometry.

3.5. Pipe Backfill Response and Highway Loads

Figure 9 shows the ultimate capacity in psf and the ultimate contact stress in psi of each soil-pipe system versus backfill density. As shown, the ultimate capacity of uncompacted till is below 9,360 psf (448 kPa) which is the lower bound of the contact stress of a typical AASHTO H-truck. Furthermore, the ultimate capacities of 80% compacted till, ISU7, and sand compacted to 96 pcf (15 kN/m^3), ISU9, are within the range of AASHTO H-truck loading. The ultimate capacity of Test ISU8 is at the upper bound of the range. If a conservative contact stress of 14,400 psf (690 kPa) for an AASHTO H-truck is used for pipe design, a minimum dry density of 110 pcf (17.3 kN/m^3) is required to prevent the localized bending failure of the pipe. This analysis is conservative

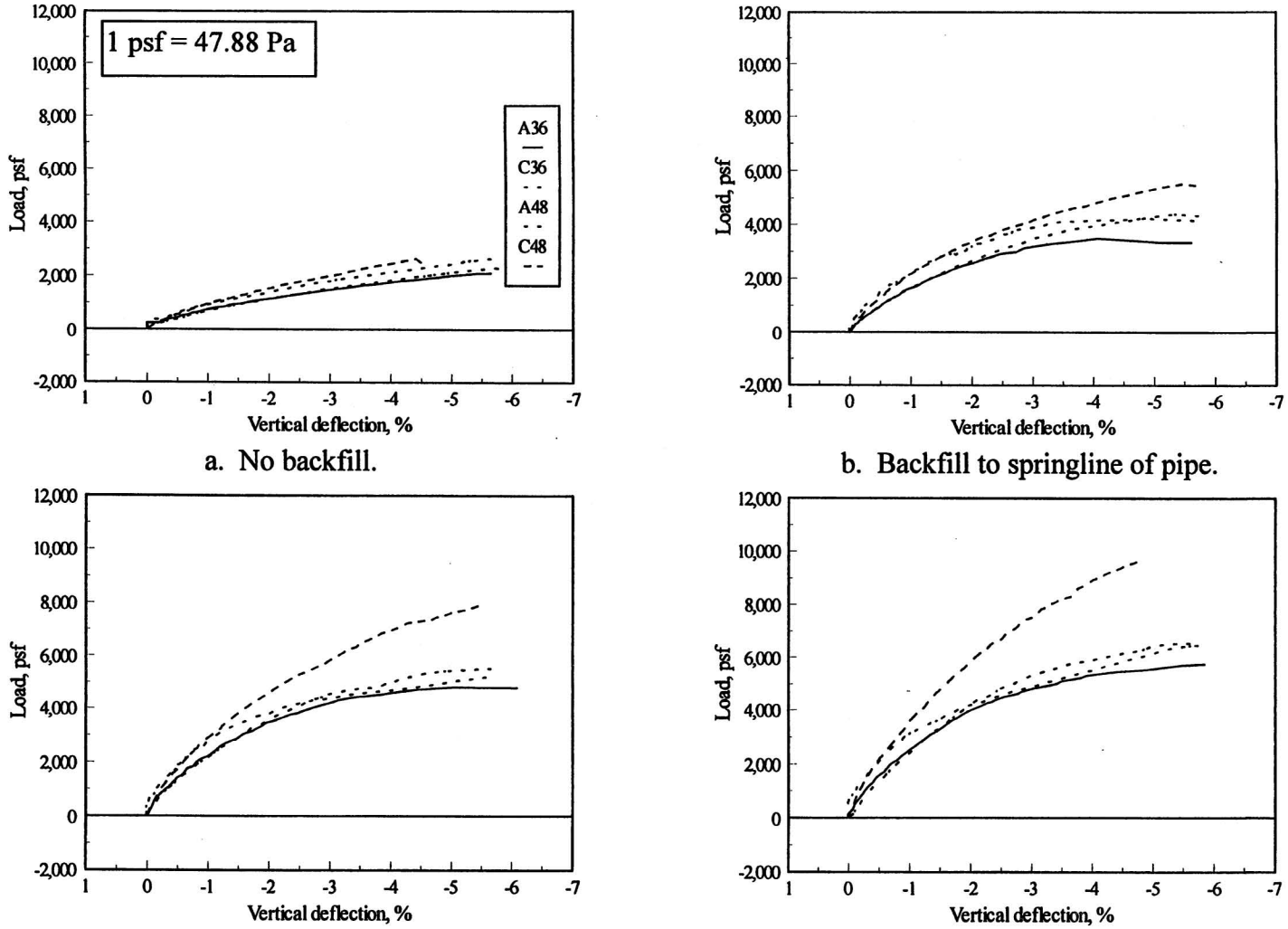

Figure 8. Changes in vertical pipe diameter as a function of backfill depth.

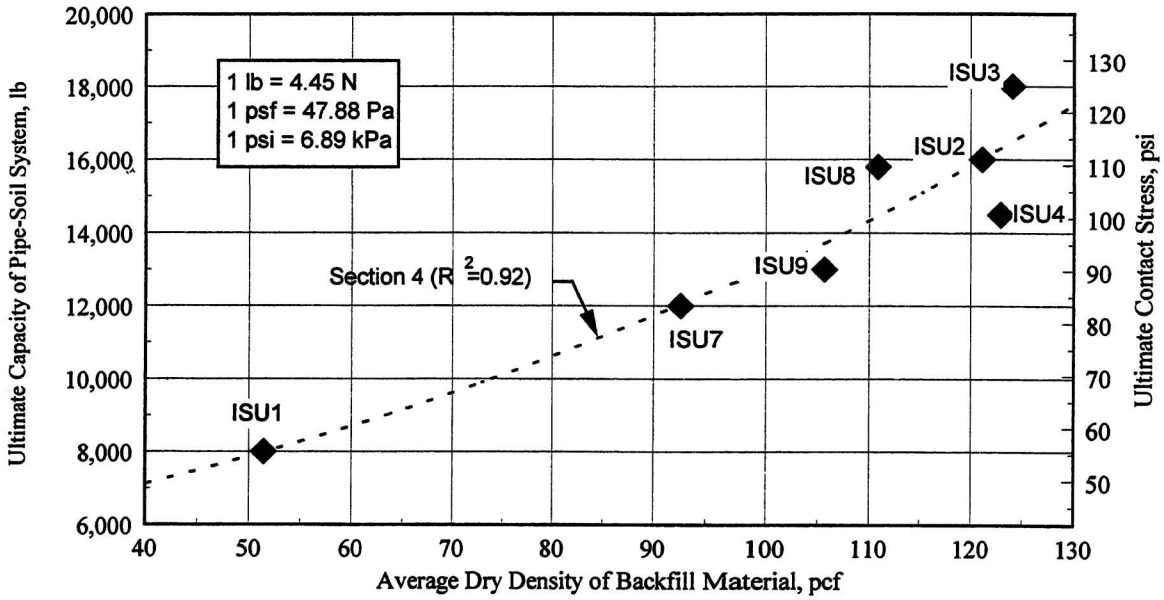

Figure 9. Ultimate capacity and ultimate contact stress of each pipe-soil system.

because of the influence of the soil bearing capacity failure caused by the load plate penetrating the soil.

3.6. Influence of Pipe Characteristics on Response to Surface Loads

Table 1 shows the relative stiffness of the pipes as measured in the parallel plate test and demonstrates that the stiffness of Pipe C is stiffer than Pipe A (for the 48 in. diameter pipe). In Figure 5 and Figure 7 where the two pipes were loaded with the 1 ft^2 (0.0093 m^2) plate but without any backfill, the data also show that Pipe C is stiffer than A. Data in Table 2 indicate that the stiffer pipe (Pipe C) was tested with the higher density backfills. In evaluating the responses of both pipes shown in Figures 2, 5, and 6 it can be seen that the stiffer pipe with better backfill exhibited smaller deflections at higher loads.

The influence of pipe stiffness is addressed in part in Figure 9 where the ultimate supporting capacity is expressed as an increase in contact stress over that of the unsupported pipe. This figure suggests that soil density contributes more to the load carrying capacity of the soil pipe system than does pipe stiffness. Increasing backfill density, throughout the range of densities studied here, increases capacities associated with localized bending failure as shown in Figures 7 and 9.

In Figure 10 the net vertical pipe deflection is plotted versus average dry density of backfill while in Figure 11 the vertical pipe deflection is normalized by dividing it by the appropriate pipe stiffness shown in Table 1. All tests reached a contact stress of 7,000 psf (335 kPa) before failure, therefore the deflections at this contact stress were used to compare the normalized response of the pipe-backfill systems. A comparison of these two figures shows that the pipe performance is less sensitive to the pipe stiffness, and more dependent on the quality of the backfill material. Both Figures 10 and 11 show that, at this low contact stress level, the vertical deflection is reduced at a higher rate with an increase from 50% standard Proctor (Test ISU1) to 80% standard Proctor (Test ISU7) than with the increase from 80% standard proctor density to 95% (Test ISU7 to Test ISU8). Also for the sand backfills at higher densities, the increase of dry density of the backfill material above approximately 110 pcf (17.3 KN/m^3) does not further reduce the vertical pipe deflection.

3.7. Pipe Response under Loads Applied near the Pipes Ends

A comparison of pipe response when loaded at the center and at the ends is discussed for Tests ISU7 through ISU13. The data presented here are consistent with Tests ISU1 through ISU4, and those data can be found in the thesis by Phares (1996). Figure 12a shows the load versus vertical deflection responses for the 36 in. (914 mm) pipes, and Figure 12b shows similar data for the 48 in. (1,220 mm) pipes. The deflections are expressed as a percentage of the pipe diameter. A

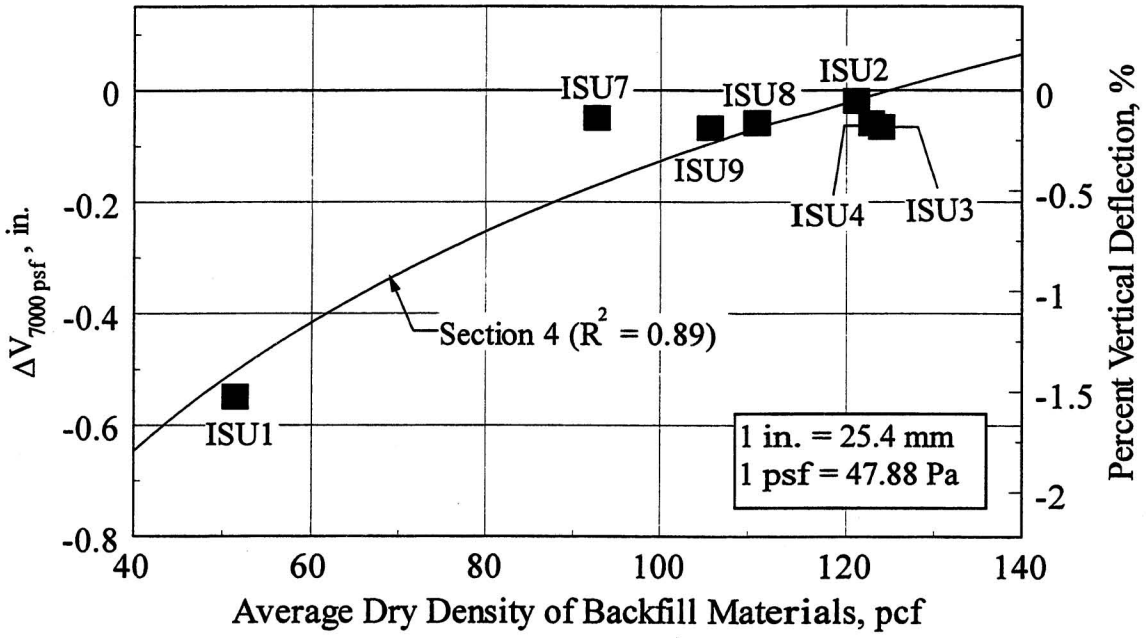

Figure 10. Net vertical diameter changes at an applied stress of 7,000 psf.

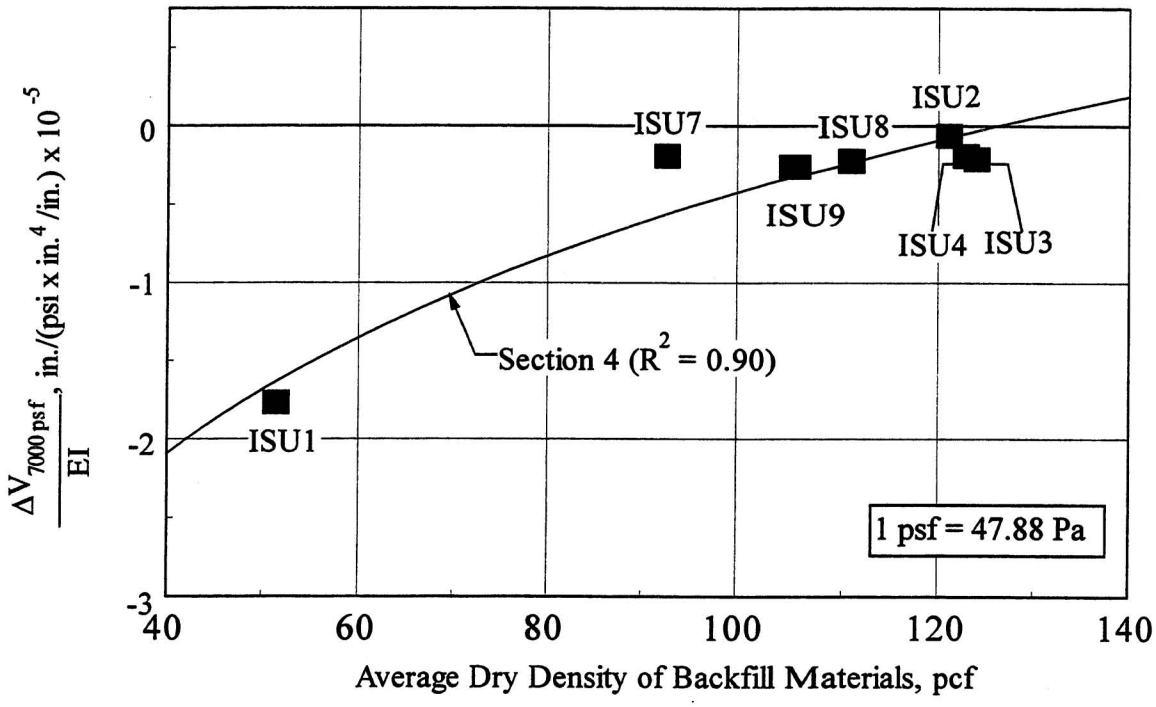

Figure 11. Net vertical diameter changes at an applied stress of 7,000 psf normalized by the pipe stiffness factor, EI.

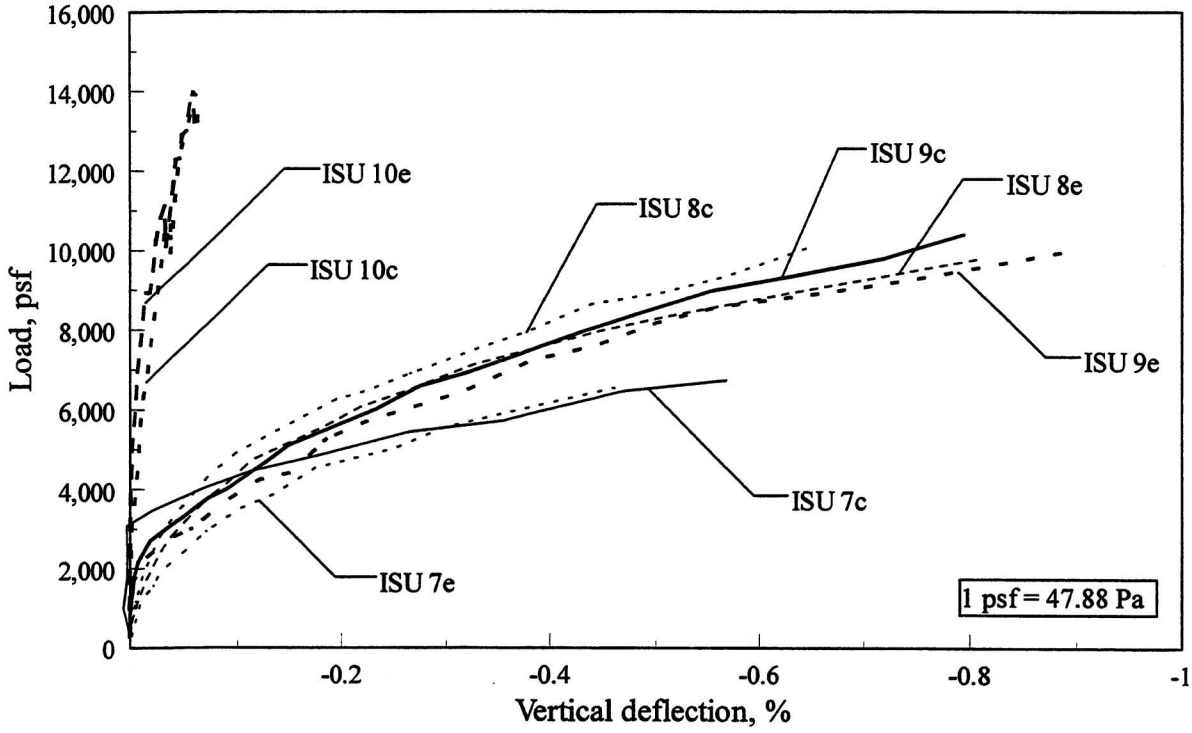

a. Service loading of 36 in. dia. pipes.

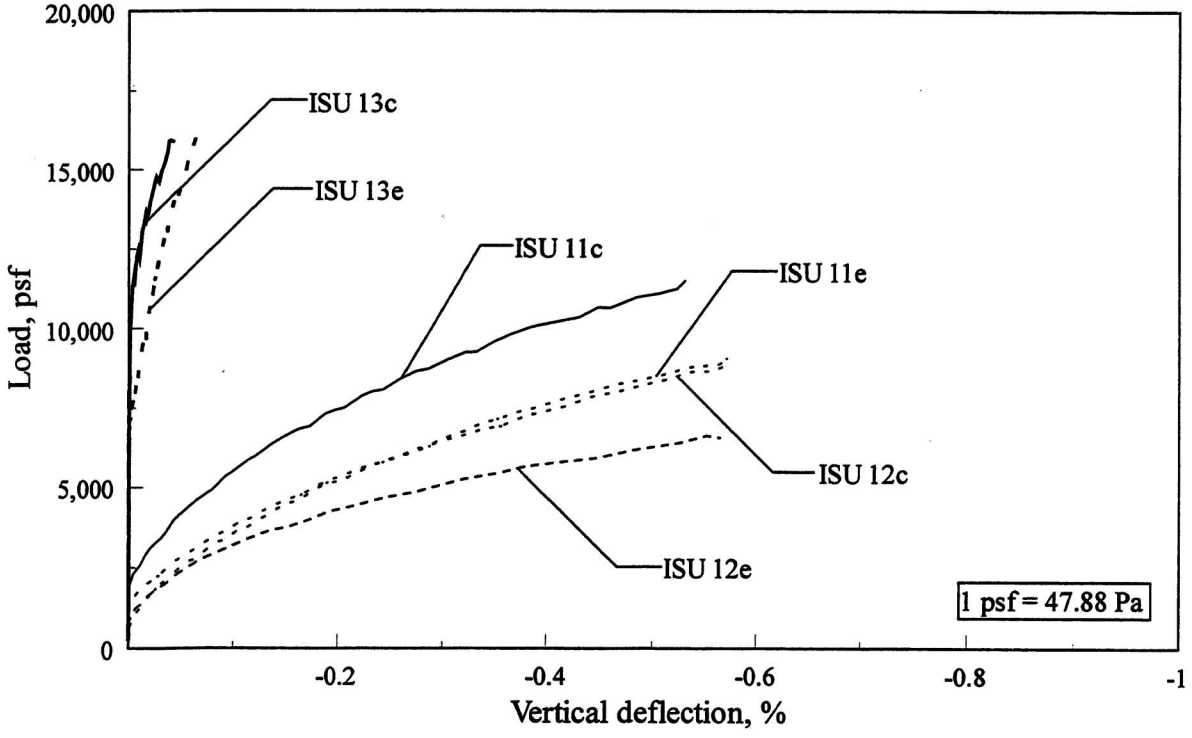

b. Service loading of 48 in. dia. pipes.

Figure 12. Percent pipe deflection during field test service loading.

comparison of the deflections at the center and the ends of the pipes in all cases shows that deflections are somewhat higher at the ends of the pipes than at the centers. (Note that the letter designation e and c for each ISU test refer to end and center, respectively). Also, the differences in deflections at the centers and ends of the pipes is larger in the larger diameter pipes. In general, the variation in deflections between the center loading and end loading in Tests ISU7 through ISU10 is small. Clearly, the flowable mortar, Test ISU10, reduces deflections at a given load by an order of magnitude while the glacial till compacted to 80% standard proctor density, Test ISU7, deforms the greatest.

In the tests on the larger diameter pipes, it can be seen that, as with the smaller diameter pipes, the flowable fill (Test ISU13) reduces deflections dramatically. Somewhat anomalous, is that the deflections of the lower density sand (Test ISU11) are less than those of the higher density backfill (Test ISU12).

In Table 4 the percent deflections at 10,000 psf (479 kPa) contact stress are compared. For pipes loaded at the center, except for the low density glacial till (Test ISU7), the percent deflections are less than 0.5%. For end loading, except for moderately high density sand (Test ISU12) and the low density till (Test ISU7) where deflections approached 2%, the percent deflections are also less than 0.5%. Except for these two tests, deflections at the end loading are about 30% higher than deflections developed under center loading. End loading of pipes with flowable fill (Tests ISU10 and ISU13) resulted in negligible deflections. In Test 12, pipe deflections from end loads are about 3 times higher than deflections from center loading. Pipe dependence on backfill may explain this result. Although the deflections are higher at the ends of the pipes, the deflections at contact stresses equivalent to moderate highway tire pressures are not excessive and the pipe-soil systems of both diameters have adequate stiffness at both the center and ends of the pipes.

3.8. Ultimate Capacity of Pipe-Soil System

Figure 13 shows the curves for loading to failure for the 36 in. (915 mm) and 48 in. (1,220 mm) pipes. Table 5 summarizes the ultimate contact stresses and failure deflections. In Figure 13, most pipe failures occurred at vertical deflection between 2 and 2.5% for loads applied at the center of the pipe. The exceptions are the pipes with the flowable fill (Tests ISU10 and ISU13) that fail at deflections of 1%. The contact stresses that cause failure of the pipes with flowable fill are more than twice the failure stresses in the pipes with soil backfill.

Table 4. Pipe deflections at 10,000 psf (479 kPa) contact surface pressure.

Field Test	Center Loading Deflection	End Loading Deflection
ISU7	1.40%	1.90%
ISU8	0.40%	0.40%
ISU9	0.40%	0.50%
ISU10	0.020%	0.050%
ISU11	0.30%	0.50%
ISU12	0.50%	1.80%
ISU13	0.010%	0.030%

When loaded at the centers of the pipes with soil backfill, except for the low density till (Test ISU7), the pipes can withstand surface contact stresses at or near expected tire pressures. The pipes with flowable fill can withstand contact stresses more than double those of the pipes with soil backfill.

Pipes that are loaded near the ends do not perform as well except for those with flowable fill backfill. Also, the larger pipe with high density sand (Test ISU12) has lower than expected

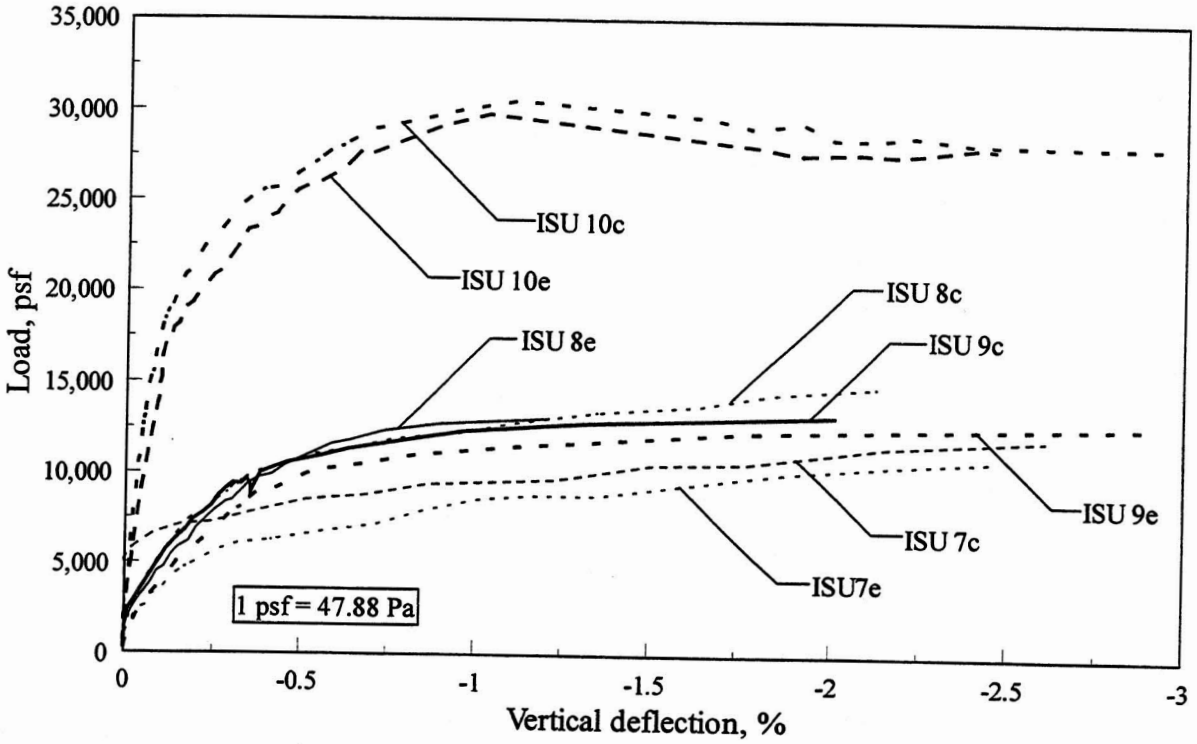

a. Failure loading of 36 in. dia. pipes.

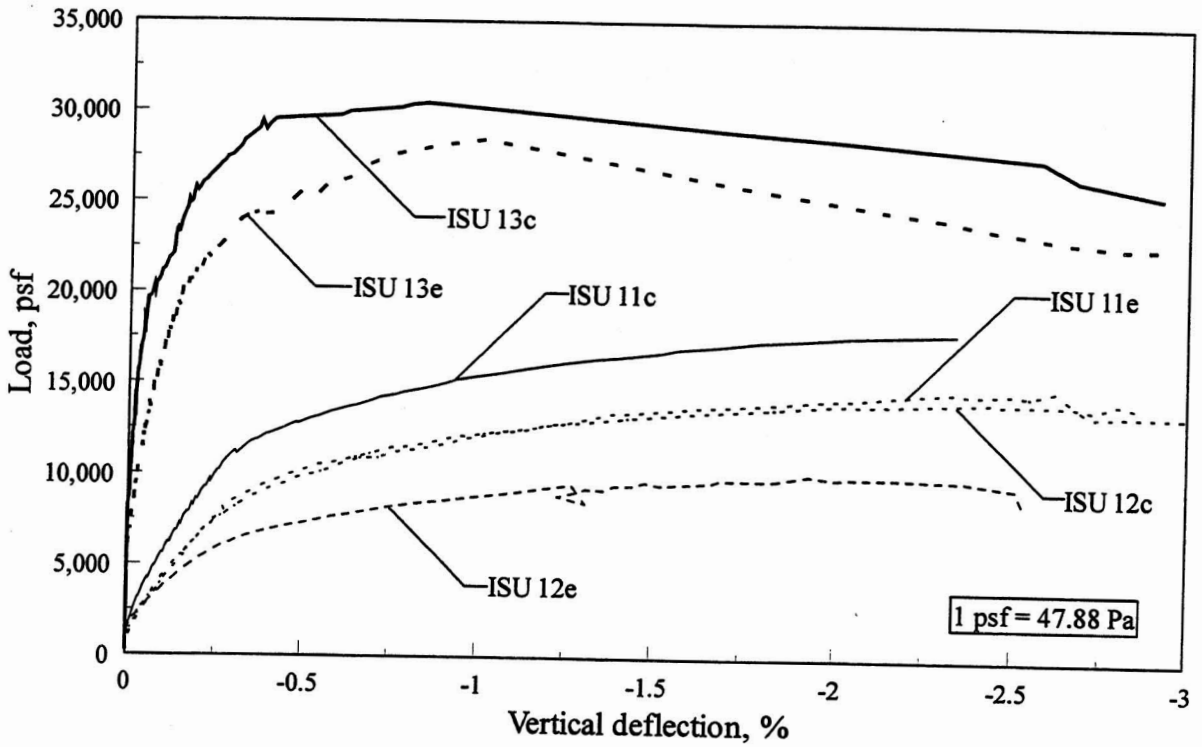

b. Failure loading of 48 in. dia. pipes.

Figure 13. Percent pipe deflection during failure loading field tests.

capacity. This is thought to be due to localized poor compaction of the soil beneath the load plate that resulted in soil bearing capacity failure.

3.9. Effect of Temperature on HDPE Pipe Strength

During the backfilling of several of the PE pipes field tested in Phase I, it was observed that the crown of the pipe was considerably hotter than the remaining portions (sides, invert, etc.) of the pipe and thus considerably more flexible. The large diameter changes and circumferential strains measured during backfilling were thought to be related to this temperature differential.

Table 5. Pipe deflections at ultimate capacity.

Field Test	Center Loading		End Loading	
	Load, psf (kPa)	Deflection	Load, psf (kPa)	Deflection
ISU7	12,000 (575)	2.60%	11,000 (525)	2.40%
ISU8	15,000 (720)	2.10%	13,000 (620)	1.20%
ISU9	13,000 (620)	2.00%	13,000 (620)	2.90%
ISU10	31,000 (1,485)	1.10%	30,000 (1,435)	1.00%
ISU11	18,000 (860)	2.30%	14,000 (670)	2.60%
ISU12	15,000 (720)	2.60%	10,000 (480)	1.90%
ISU13	30,000 (1,435)	0.80%	28,000 (1,340)	1.00%

Once the pipe was buried, the soil insulated the pipe thereby eliminating the temperature differential. To investigate the effect of temperature variation on the load-deflection behavior of PE pipe, a limited number of parallel plate tests were conducted in which various regions of the pipes were heated (to simulate the effect of the sun on pipe in the field). These specimens as

well as some of the field tests were instrumented so that strains, diameter changes and temperature distributions could be measured.

3.9.1. Parallel Plate Testing

The parallel plate testing program consisted of placing pipe specimens between two rigid plates and applying a line load at an ASTM prescribed controlled loading rate to the specimens. Parallel plate tests were performed at ambient and at elevated temperatures. Temperature effects were introduced using heat lamps creating temperature gradients similar to the conditions that may occur during field installation of the pipe during the summer. It was observed during the field tests that the crown of the pipe reached surface temperatures of approximately 120°F (50°). The test specimens were enclosed in an insulated box. The instrumentation used in these tests and the orientation of the heat lamps is shown in Figure 14.

For each specimen tested, the temperature distribution around the pipe, changes in vertical and horizontal diameters, and circumferential strains were recorded. Also, pipe stiffness was calculated at 5% deflection according to ASTM D2412.

A total of 4 specimens (A36, A48, C36, C48) were tested. Parameters of each specimen are presented in Table 6.

The testing program included four parallel plate tests to 5% deflection on each specimen. One test was conducted at ambient air temperature and three tests were performed at elevated temperatures, varying heat lamp locations around the pipe as shown in Figure 14.

As shown in Figure 14, each test specimen was instrumented with four strain gages, four deflection transducers, and eight thermocouples. All instrumentation was placed at the center of the specimens on the inside pipe surface.

Strain gages were oriented in the circumferential direction. Two deflection transducers

were used to measure changes in the vertical and horizontal diameters; the eight thermocouples were installed at 45° intervals around the circumference of pipe specimens to measure temperature distribution.

Table 6. Properties of parallel plate specimens tested.

Manufacturer	Inside Diameter		Specimen	
	Nominal, in. (mm)	Actual, in. (mm)	Wall thickness, in. (mm)	Length, in. (mm)
A36	36 (915)	35.81 (910)	0.234 (6)	37.21 (945)
A48	48 (1,220)	47.92 (1,215)	0.297 (8)	46.75 (1,185)
C36	36 (915)	35.89 (910)	0.292 (7)	36.08 (915)
C48	48 (1,220)	47.07 (1,195)	0.180 (5)	51.43 (1,305)

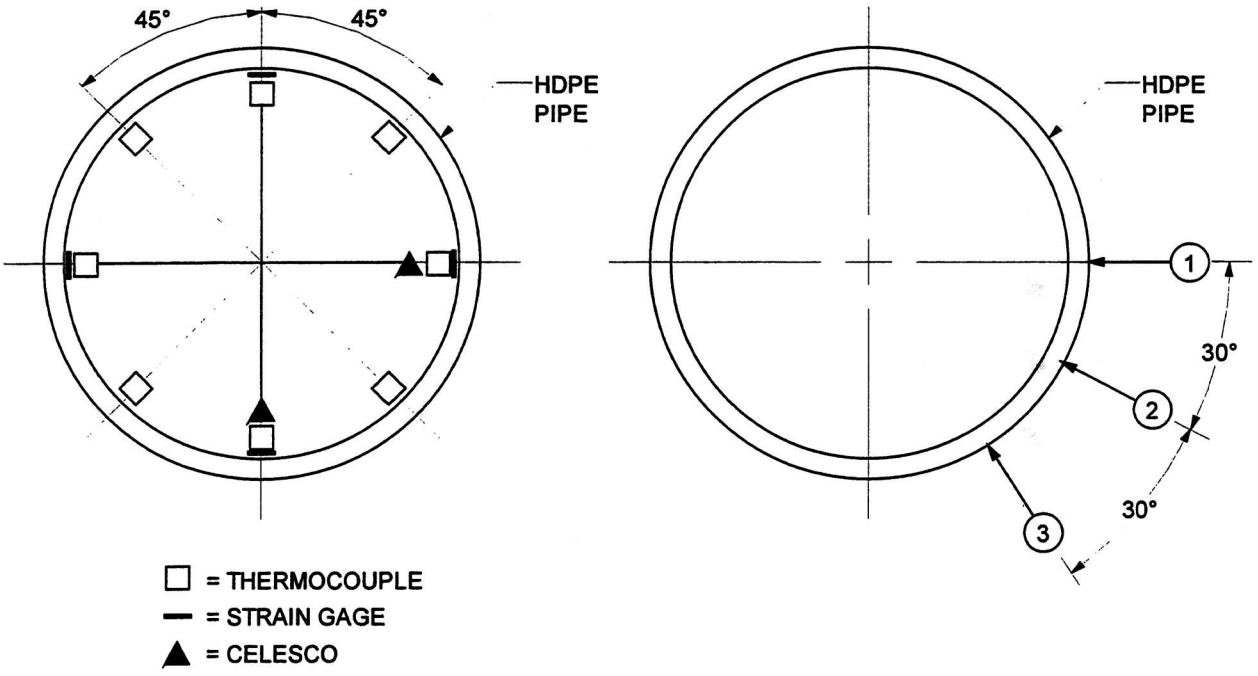

a. Instrumentation

b. Location of heat lamps

Figure 14. Details of instrumentation and location of heat lamps used in parallel plate tests.

In the field tests, in addition to the instrumentation described in Sec. 2.3, several specimens were instrumented with thermocouples to record pipe temperatures during backfilling. Tests during the summers of 1996 and 1997 were conducted on relatively cool days, thus no pertinent temperature data were obtained.

3.9.2. Pipe Stiffness Results

Pipe stiffness per ASTM D2412 is defined as the force per unit length of the specimen divided by the resulting deflection obtained at a specified percentage of pipe deflection. Pipe stiffness was calculated at 5% deflection for all parallel plate tests performed in this phase of the project. Pipe stiffnesses and the highest inside surface temperature that occurred during testing of the various specimens is presented in Table 7. At elevated temperatures, a decrease in pipe stiffness of approximately 30% occurred in the 36 in. (915 mm) diameter specimens and a decrease of approximately 37% occurred in the (48 in.) diameter specimens. A significant decrease in pipe stiffness at temperatures in the range of 68-86∘F (20-30∘C) above ambient room temperatures occurred.

According to AASHTO, the minimum requirements for pipe stiffness at 5% deflection on 36 and 48 in. (915 and 1,220 mm) diameter flexible pipes are 22 and 18 psi (150 and 125 kPa), respectively. All specimens tested at ambient room temperature conform to this minimum requirement; however, all specimens at elevated temperatures except heat lamp orientation 1 and 2 on specimen A36 failed to meet this requirement. This result implies that some HDPE, installed on hot summer days, pipes may not meet AASHTO minimum pipe stiffness requirements.

During testing, horizontal and vertical deflection transducers were monitored during loading. The load-deflection response of all four specimens tested in this phase of the project as a

function of heat lamp orientation was measured. Shown in Figure 15 is the load-deflection response of specimen A48. As may be seen in this figure, testing at elevated pipe temperatures produced higher deflections at lower loads; however, heat lamp orientation had minimal effect on the deflection response. Heating any portion of the pipe circumference reduced the load

Table 7. Pipe stiffnesses at ambient and elevated temperatures determined using ASTM D2412.

Manufacturer	Diameter, in.	Description	Temperature, °F	Pipe Stiffness at 5% Deflection, psi (kPa)
C	36	Ambient	72 (22)	35.80 (245)
		Orientation 1	113 (45)	27.34 (190)
		Orientation 2	115 (46)	27.39 (190)
		Orientation 3	115 (46)	21.58 (150)
A	36	Ambient	72 (22)	29.99 (205)
		Orientation 1	115 (46)	21.58 (150)
		Orientation 2	115 (46)	19.76 (135)
		Orientation 3	118 (48)	20.15 (140)
C	48	Ambient	77 (25)	22.46 (155)
		Orientation 1	111 (44)	14.62 (100)
		Orientation 2	113 (45)	14.24 (100)
		Orientation 3	113 (45)	16.05 (110)
A	48	Ambient	72 (22)	20.62 (140)
		Orientation 1	122 (50)	13.04 (90)
		Orientation 2	118 (48)	12.90 (90)
		Orientation 3	120 (49)	13.38 (90)

carrying capacity of HDPE pipes. Similar behavior was found for all specimens; for additional information on this phase of the investigation the reader is referred to Conard *(1997)*.

Circumferential strain data were collected at four locations on the inside surface of pipe specimens to study the strain response of HDPE pipes in ring compression. For specimen A48 shown in Figure 16 (see Figure 17 for the key describing the location of the various circumference strains), elevated temperatures produced higher strains for a given load.

Heat lamp orientation 1, which is similar to the condition that would occur in the field during backfilling, generally produced higher strains for a given load in all the pipes tested. However, any heat lamp orientation produced somewhat higher strains than those at ambient temperatures. This indicates that the circumferential strain response is sensitive to temperature; this sensitivity was also observed in the deflection responses. From this investigation, it appears that the circumferential response of HDPE pipe is temperature sensitive but the location of heat source has minimal effect on pipe response in the circumferential direction.

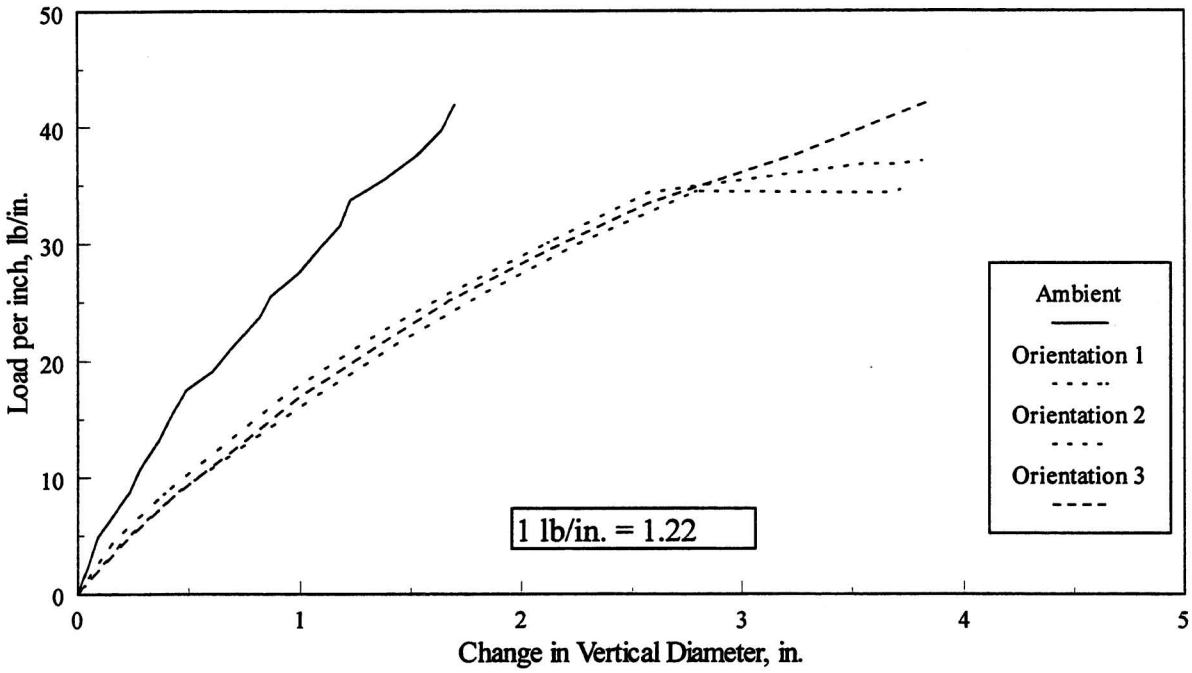

a. Vertical deflection.

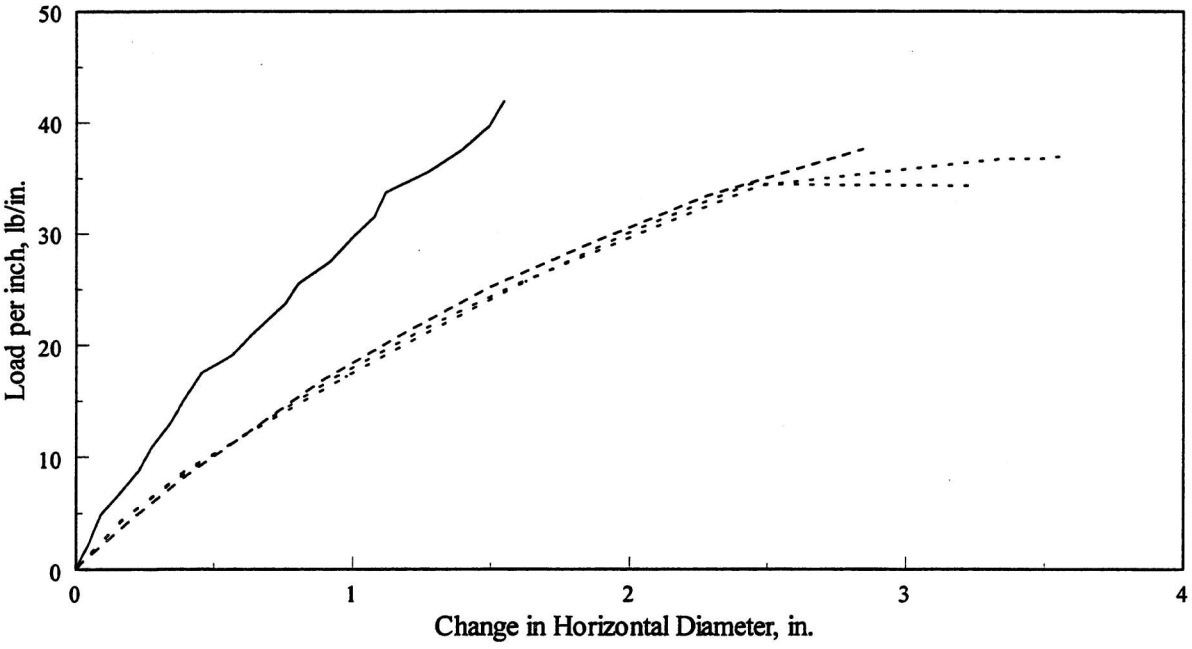

b. Horizontal deflection.

Figure 15. Load versus change in pipe diameter: Specimen A48.

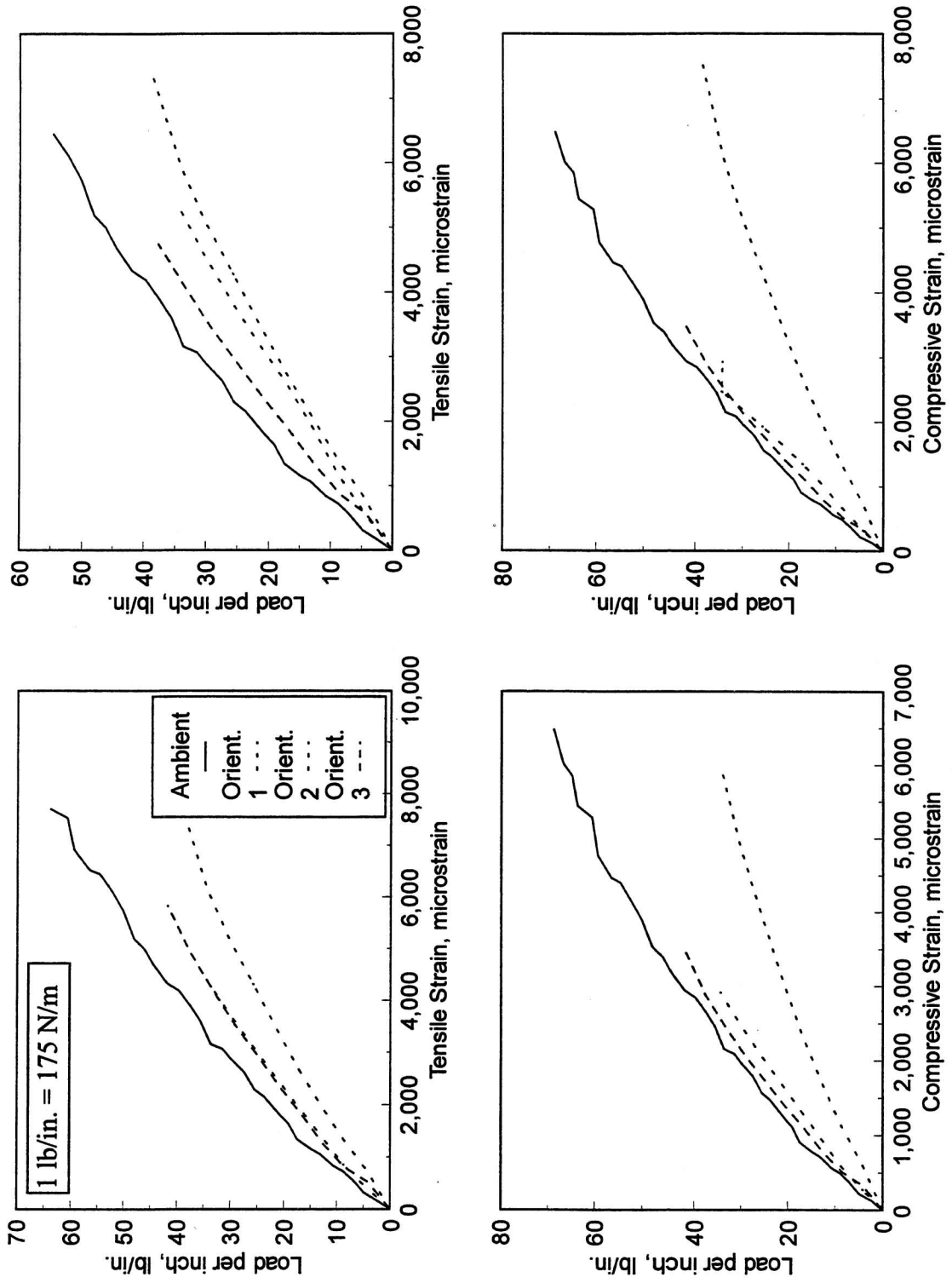

Figure 16. Load versus circumferential strain: Specimen A48.

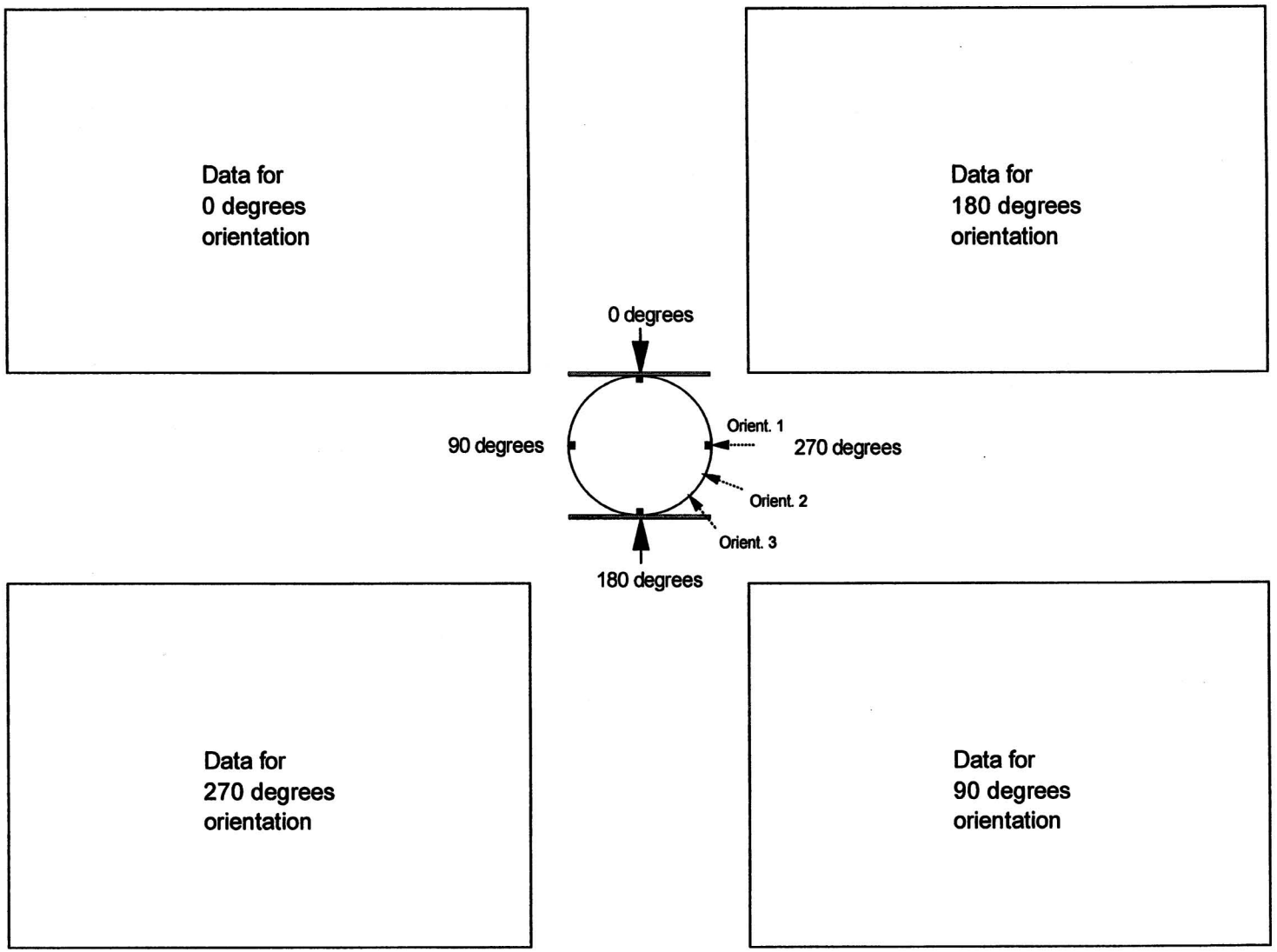

Figure 17. Key for strains presented in Figure 16.

4. NUMERICAL ANALYSIS USING Culvert ANalysis and DEsign (CANDE)

4.1. General Background

Culvert ANalysis and DEsign (CANDE) is a finite element computer program developed for structural design and analysis of buried culverts. As described by Musser *(1989)*, CANDE methodology combines the culvert structure with the soil mass into an incremental, static, plane-strain boundary value problem. Katona *(1976)* stated that the more significant limitations and deficiencies of CANDE are small displacement theory, time independence, and out-of-plane effects. Four criteria are considered for plastic pipe design by CANDE including pipe deflections, outer fiber stresses, buckling pressures, and handling performance.

In the CANDE library, a choice of three solution levels, five types of pipe, and six soil constitutive models are available for matching the degree of analytical power to the problem at hand. The solution level 1 is an elastic method that is restricted to circular pipes deeply buried in a homogeneous soil with a uniformly applied pressure acting on horizontal planes. The schematic model of solution level 1 is show in Figure 18. The solution levels 2 and 3 is based on incremental virtual work using a displacement formulation. Level 2 generates the user defined finite element mesh automatically; however, level 3 requires the user to create and define the mesh topology. The solution level 2 generates an axisymmetrical model (only the right half system is modeled); however, solution level 3 provides nearly unlimited modeling flexibility including full meshes or half meshes for any shaped culvert. In addition, the extended level 2 option allows the user to selectively change the level 2 mesh to match the problem conditions. The schematic trench model of solution level 2 is shown in Figure 19.

The five pipe types are aluminum, basic, concrete, plastic, and steel, and only one pipe type is selected for a given problem. Each pipe type is generated in a separate subroutine and has its own stress-strain model and design/evaluation logic. The pipe materials stated above are

self explainable except the basic pipe type. The basic pipe model permits the user to describe nonstandard materials (or built-up) pipe properties.

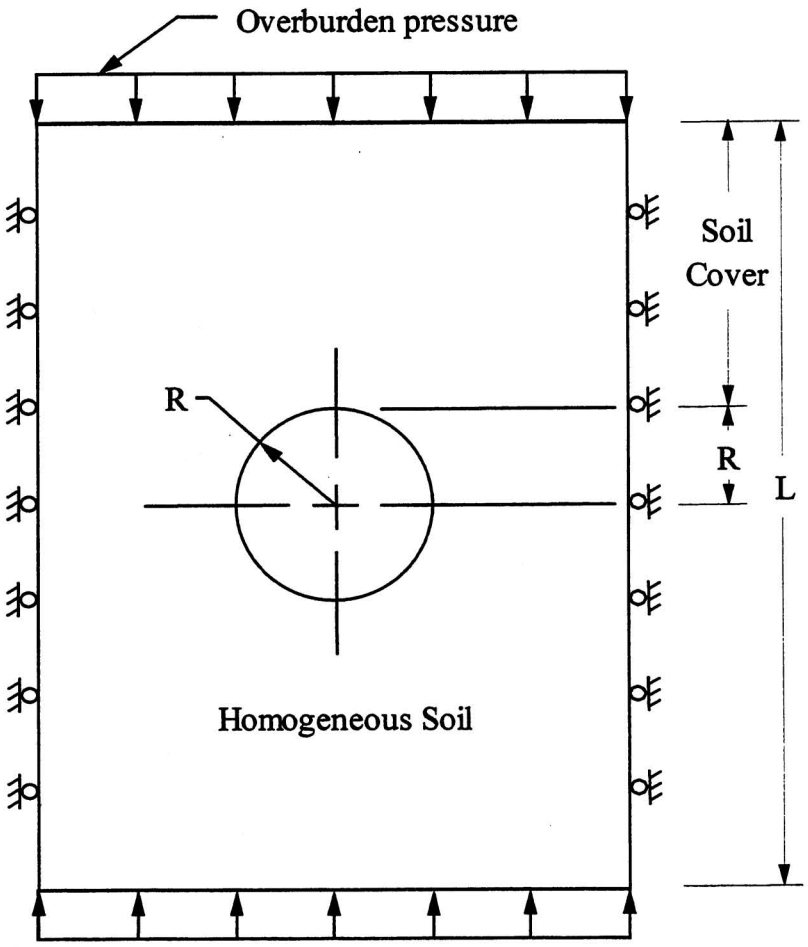

Figure 18. The schematic model of solution level 1.

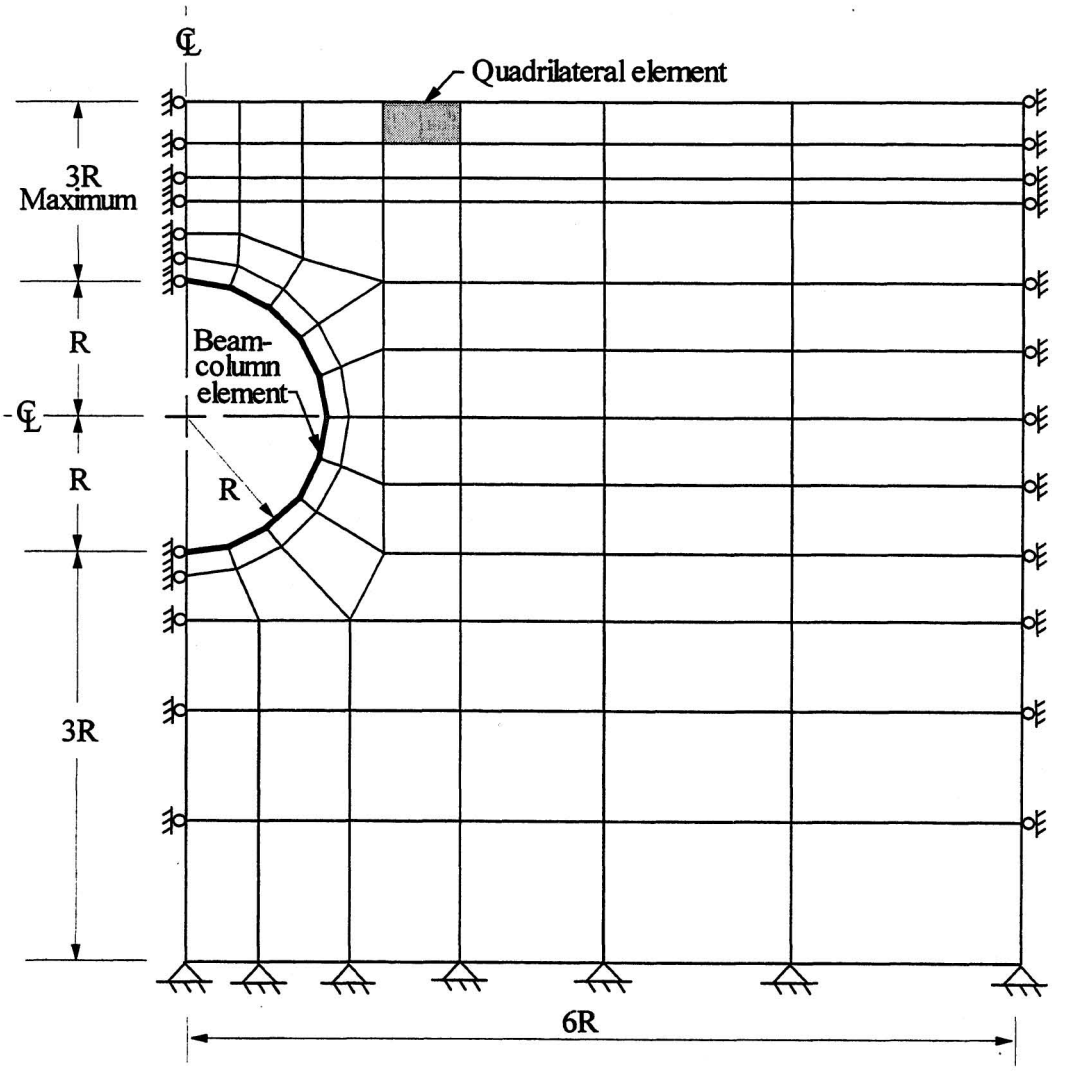

Figure 19. The schematic trench model of solution level 2.

The six soil constitutive models currently available in CANDE are isotropic linear elastic, orthotropic linear elastic, overburden dependent, Hardin, Duncan, and Selig. The isotropic linear elastic model is defined by Young's modulus and Poisson's ratio. The orthotropic linear elastic model is applicable to directional dependent behavior in engineering materials. If a soil element is confined and the deformations are primarily in one direction, the overburden dependent model which is defined by overburden stress dependent Young's modulus and Poisson's ratio can be

applied. The Hardin model is defined by a variable shear modulus and a variable Poisson's ratio. Duncan model is defined by a variable Young's modulus and a variable bulk modulus; it is particularly suited to incremental construction simulation and characterizing compacted soils in zones of soil-structure interaction. The Selig model which is an extension of Duncan model uses the same Young's modulus formulation but with an alternative bulk modulus having a hyperbolic formulation. A library of the soil parameters of each soil model can be found in the *CANDE-89 User Manual* by Musser *(1989)*.

Three basic element types used in solution levels 2 and 3 are quadrilateral (or triangular) elements, beam-column elements, and interface elements. Quadrilateral elements have four external nodes and two translational degrees of freedom per node. Beam-column element is a straight, line-shaped element with a node at each end; each node has three degrees of freedom - two translations and a rotation. Each culvert structure is formed by connecting the beam-column elements end-to-end. An interface element is composed of three nodes; two of the nodes belong to the respective subsystems on either side of the interface, and the third node is an "interior" node associated with interface forces. A pictorial description of the beam-column and quadrilateral elements is shown in Figure 2. Detailed descriptions of CANDE can be found in Katona *(1976)* and Musser *(1989)*.

4.2. Objective and Scope

The objective of this study was to use CANDE to simulate the static interaction of pipe structures and the surrounding soil under surface loads. The main purpose of this theoretical analysis was to establish minimum soil cover heights required to safely support typical AASHTO H-truck tire loads for various types and diameters of high density polyethylene

(HDPE) corrugated plastic pipes. Several soil conditions with different soil compactions and soil types were investigated.

Before computing the minimum depth of soil cover, the analytical pipe data presented by Katona *(1990)* were used to validate the method of analysis and analytical assumptions used in this study. Using the same methodology and the analytical assumptions, models were developed to simulate and compare with the field test results of ISU4, ISU8, and ISU9. Finally, minimum cover height tables were developed for both 36 in. (915 mm) and 48 in. (1,220 mm) pipes (from both Manufacturers A and C) as a function of soil quality and pipe stiffness.

4.3. Validation of Methodology

Because CANDE is based on a two-dimensional geometry called plane-strain, the three-dimensional effect of truck loads on the soil surface cannot be simulated directly. To simulate the truck loads in two dimensions, an approximate analytical method suggested by Katona *(1976)* was used to represent a single concentrated point load, Q, by an "equivalent" strip load, q, that can be handled by CANDE (see Figure 20). The strip load, q, is actually referred to a line load. This approximation is based on equating vertical stresses (at the pipe crown) between Boussinesq's elastic theories for concentrated and strip loadings. The "equivalent" strip load, q, is expressed as:

$$q = \frac{3}{4}\left(\frac{Q}{L}\right)$$

where

q = An "equivalent" strip load, lb/in.
Q = A concentrated load, lb.
L = The shortest distance from the point load to the pipe crown, in.

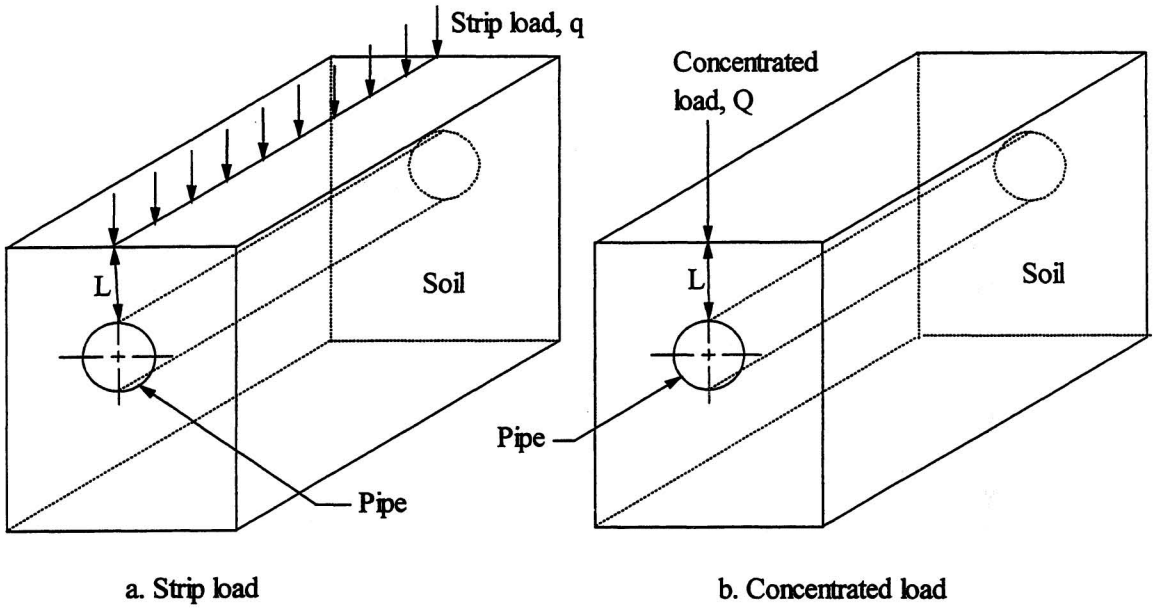

Figure 20. Loading conditions of a strip load, q, and a concentrated load, Q.

Katona *(1990)* presented analytical results on 24 in. (610 mm) HDPE pipes with a 12 in. (305 mm) soil cover using CANDE to demonstrate how the vertical pipe deflections are influenced by the soil quality. He modeled the pipe with a connected sequence of beam-column elements and the soil with continuum elements by using a revised Duncan hyperbolic soil model. The fundamental assumptions were small deformation theory, linear elastic polyethylene properties, and a bonded pipe-soil interface. The engineering properties of the pipes he used are summarized in Table 8. Silty clayey sand at 85% standard Proctor (SC85) and silty clayey sand at 100% standard Proctor (SC100) were used in the analysis; their Duncan model parameters are summarized in Table 9.

Table 8. Polyethylene material properties of 24 in. (610 mm) HDPE pipes used by Katona *(1990)*.

	Young's Modulus (Short Term), psi (MPa)	Design Strength (Short Term), psi (MPa)	Area, $in^2/in.$ (mm^2/mm)	Moment of Inertia, $in^4/in.$ (mm^4/mm)	Corrugated Height, in. (mm)
24 in. HDPE Pipe	110,000 (760)	3,000 (20)	0.3 (8)	0.18 (2,950)	2.0 (51)

Table 9. Duncan model parameters of SC85 and SC100.

Soil Name	Soil Type	AASHTO T-99, %	ϕ_o (deg)	$\Delta\phi$ (deg)	C, Psi (kPa)	K	n	R_f	K_b	M
SC85	SC	85	33	0	1.39 (9.6)	100	0.6	0.7	50	0.5
SC100	SC	100	33	0	3.47 (24)	400	0.6	0.7	200	0.5

Based on the approximate analytical method suggested by Katona *(1976)* and his analytical results Katona *(1990)*, a similar finite element model was developed by the authors in an attempt try to obtain the same pipe responses. The same pipe, soil models, and soil properties were used; also the same fundamental analysis assumptions were made. The schematic diagram of the finite element mesh is shown in Figure 21. Each CANDE solution was obtained by first applying the soil loading followed by five increments of surface live load pressure up to 50 psi (345 kPa) and 100 psi (690 kPa) for SC85 and SC100, respectively. The five increments of surface live load pressure were chosen to simplify the computations. Note that the strip load used in the input file is equal to one half of the "equivalent" strip load, q, because the finite element model is symmetrical about the vertical axis through the center of the pipe. The comparisons between the vertical deflections obtained from the finite element model shown in

Figure 21 and the analytical data presented by Katona *(1990)* are presented in Figure 22. As may be seen in this figure, there is good agreement between Katona's deflection and the analytical

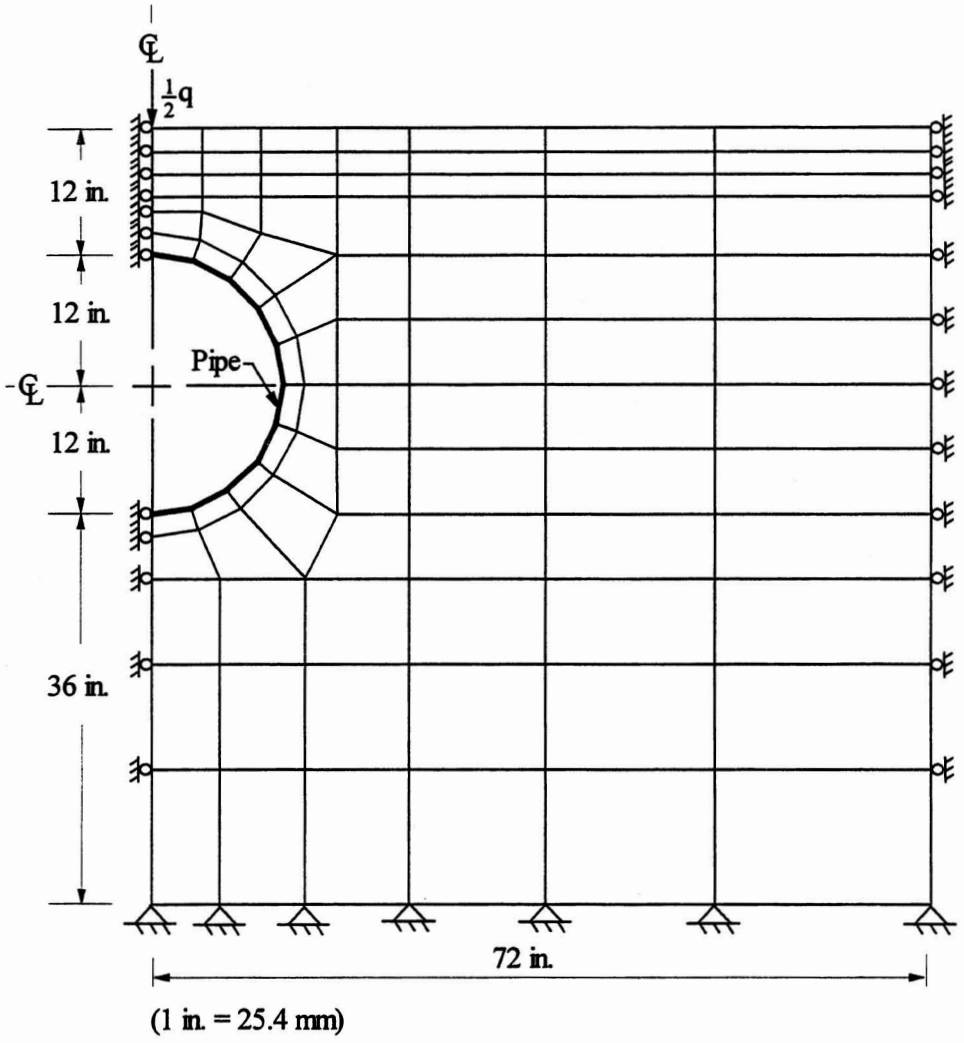

Figure 21. Schematic diagram of the finite element mesh of a 24 in. pipe for comparison with Katona *(1990)*.

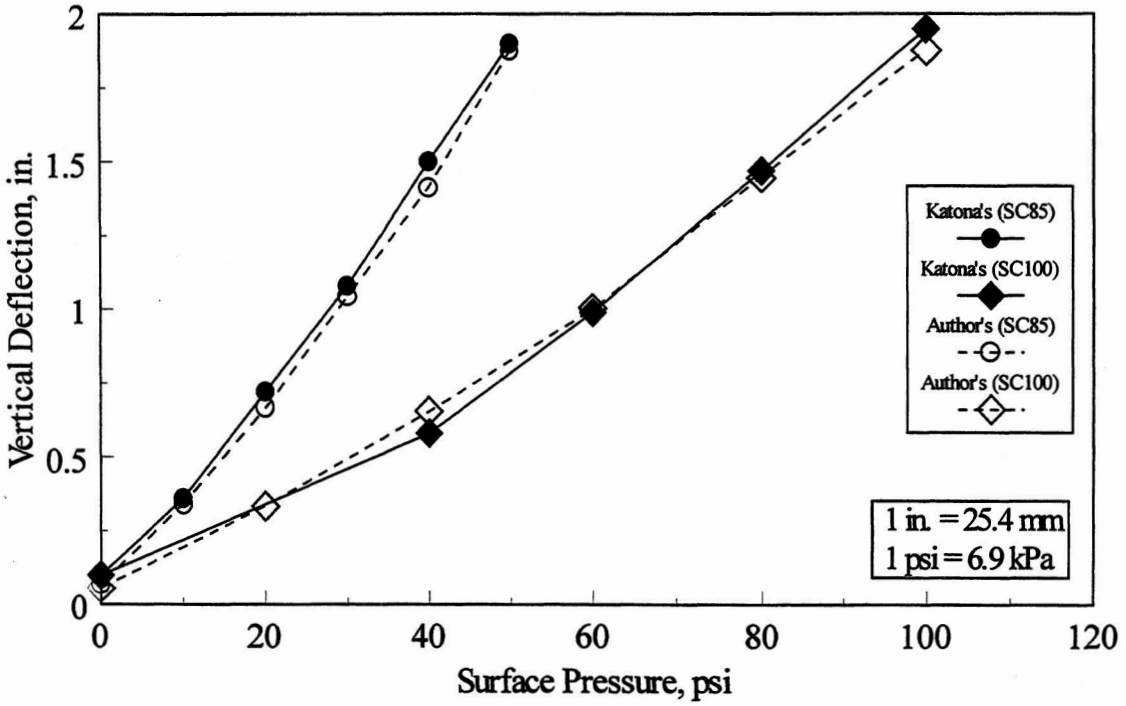

Figure 22. Comparison between Katona's and author's analytical data.

deflection obtained in this investigation for both soil cases, SC85 and SC100. This agreement validates the analytical methodology developed by the authors. The analyses presented in the next sections are based on this analytical methodology and the aforementioned assumptions.

4.4. Comparison of Analysis with Experimental Data

Experimental data from field tests ISU4, ISU8, and ISU9 were compared with the analytical data from CANDE. The purpose of these field tests was to determine the live load deflection of the HDPE pipes as a function of soil quality and pipe stiffness. As previously noted, each pipe specimen was buried with a 24 in. (610 mm) soil cover. Field test ISU4 completed by Klaiber et al. *(1996)* was performed on 36 in. (915 mm) HDPE pipe from Manufacturer C. It was backfilled with sand in three lifts to 70% of the pipe diameter, and the remainder of the backfill used glacial till. Field test ISU8 completed in this phase was performed

on 36 in. (915 mm) HDPE pipe from Manufacturer A. It was backfilled entirely with 95% compacted glacial till. Field test ISU9 has the same backfill profile as ISU4, but it was performed on 36 in. (915 mm) HDPE pipe from Manufacturer A.

A finite element model using CANDE was developed for each field test. The differences between each model were the pipe properties and the backfill conditions (i.e., different Duncan soil parameters). The pipe properties that were given by the manufacturers are summarized in Table 10. The finite element mesh generated using the extended level 2 for all the field tests is shown in Figure 23. The finite element models of the field tests ISU4, ISU8, and ISU9 with the corresponding backfill conditions are shown in Figures 24, 25, and 26, respectively. The nomenclature of the surrounding soil is presented as its Unified classification followed by its percent compaction. The Duncan soil parameters of the surrounding soil are selected from the *CANDE-89 User Manual* (Musser, *1989*) summarized in Table 11. The analytical and the experimental vertical pipe deflections of ISU4, ISU8, and ISU9 are shown in Figures 27, 28, and 29, respectively. The experimental vertical pipe deflections are the measured deflections at Section 4 (mid-point) of the pipes under the 12 in. (305 mm) square loaded plate.

Table 10. Manufacturer's polyethylene material properties of 36 in. (915 mm) and 48 in. (1,220 mm) HDPE pipes which were field tested.

Pipe	Young's Modulus (Short Term), psi (MPa)	Design Strength (Short Term), psi (MPa)	Possion's ratio, in./in.	Moment of Inertia, $in^4/in.$ (mm^4/mm)
A36	110,000 (760)	3,400 (25)	0.45	0.506 (8,290)
C36	110,000 (760)	3,400 (25)	0.45	0.55 (9,015)
A48	110,000 (760)	3,400 (25)	0.45	0.692 (11,340)
C48	110,000 (760)	3,400 (25)	0.45	0.74 (12,126)

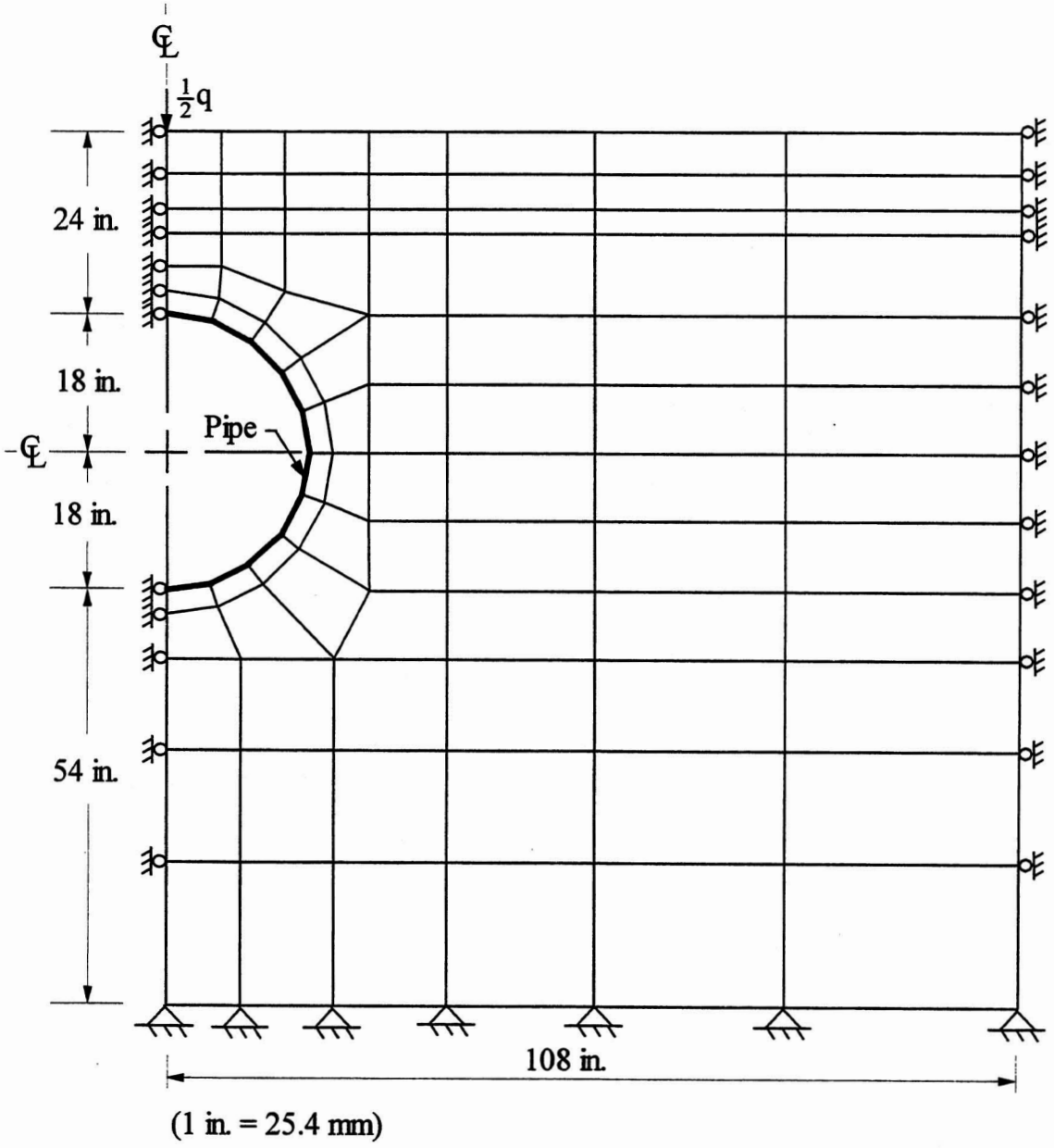

Figure 23. Schematic diagram of the typical finite element mesh of the 36 in. pipe used for comparison with field test data.

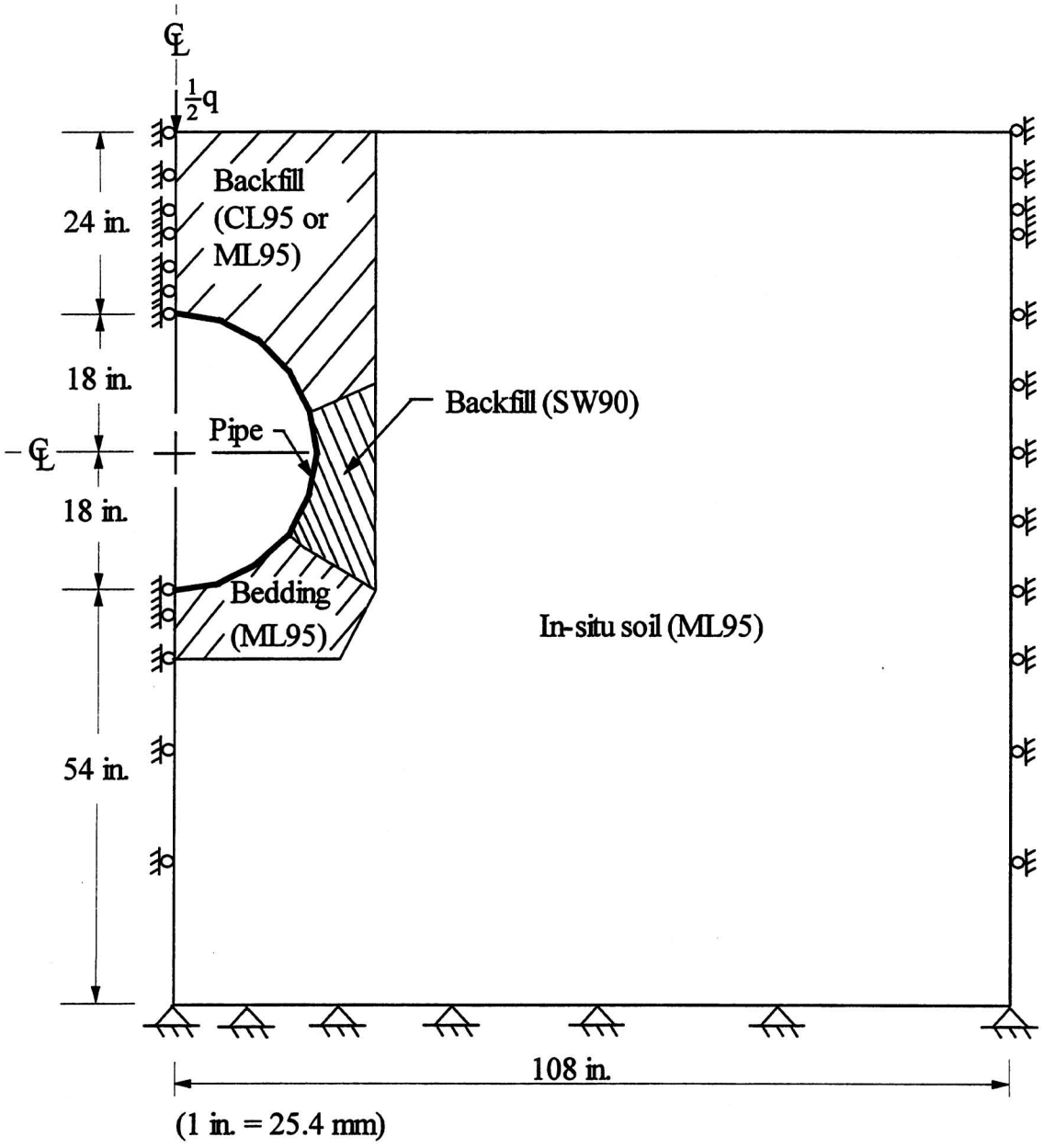

Figure 24. The finite element model of field test ISU4 (mesh shown in Figure 23).

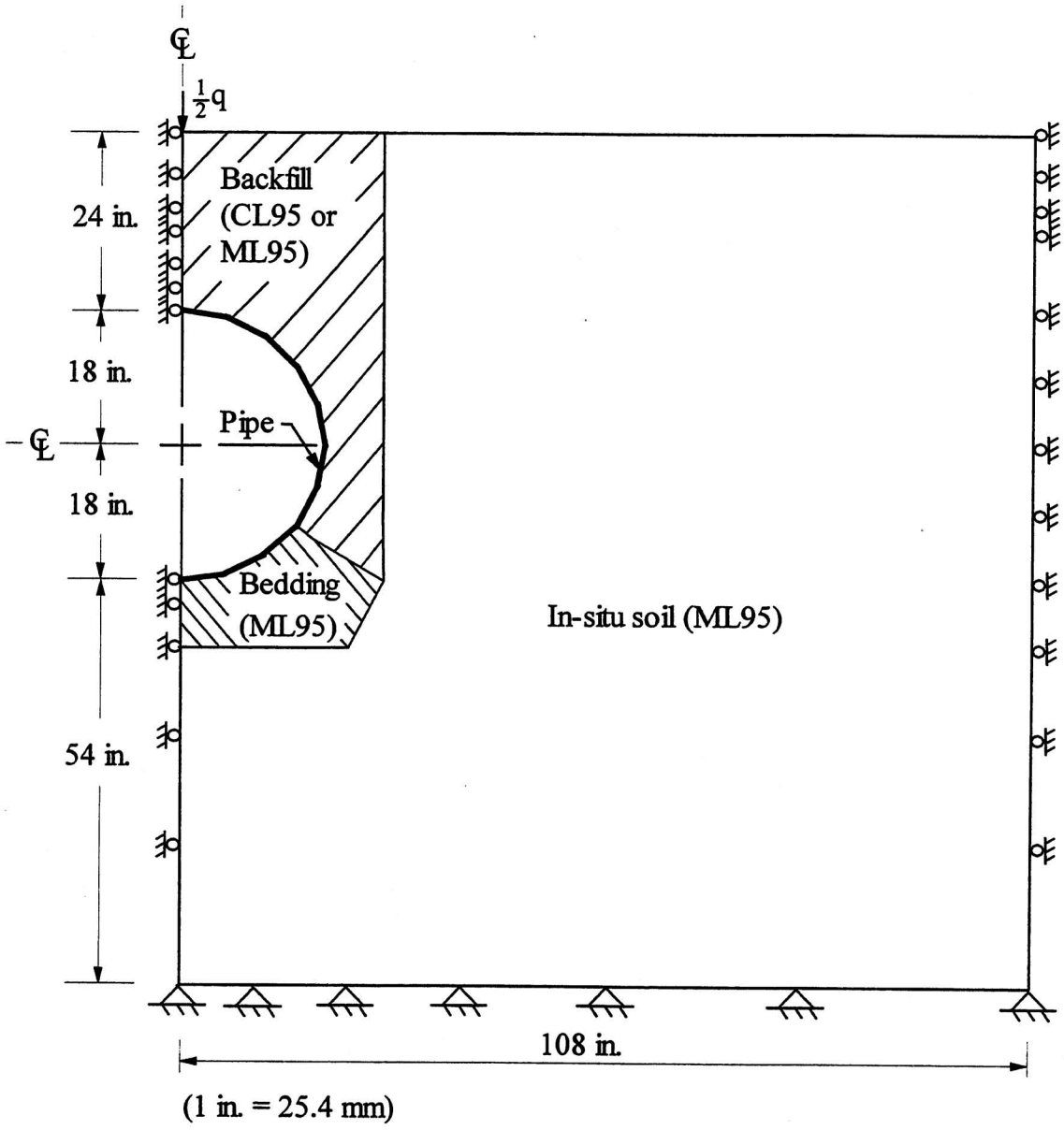

Figure 25. The finite element model of field test ISU8 (mesh shown in Figure 23).

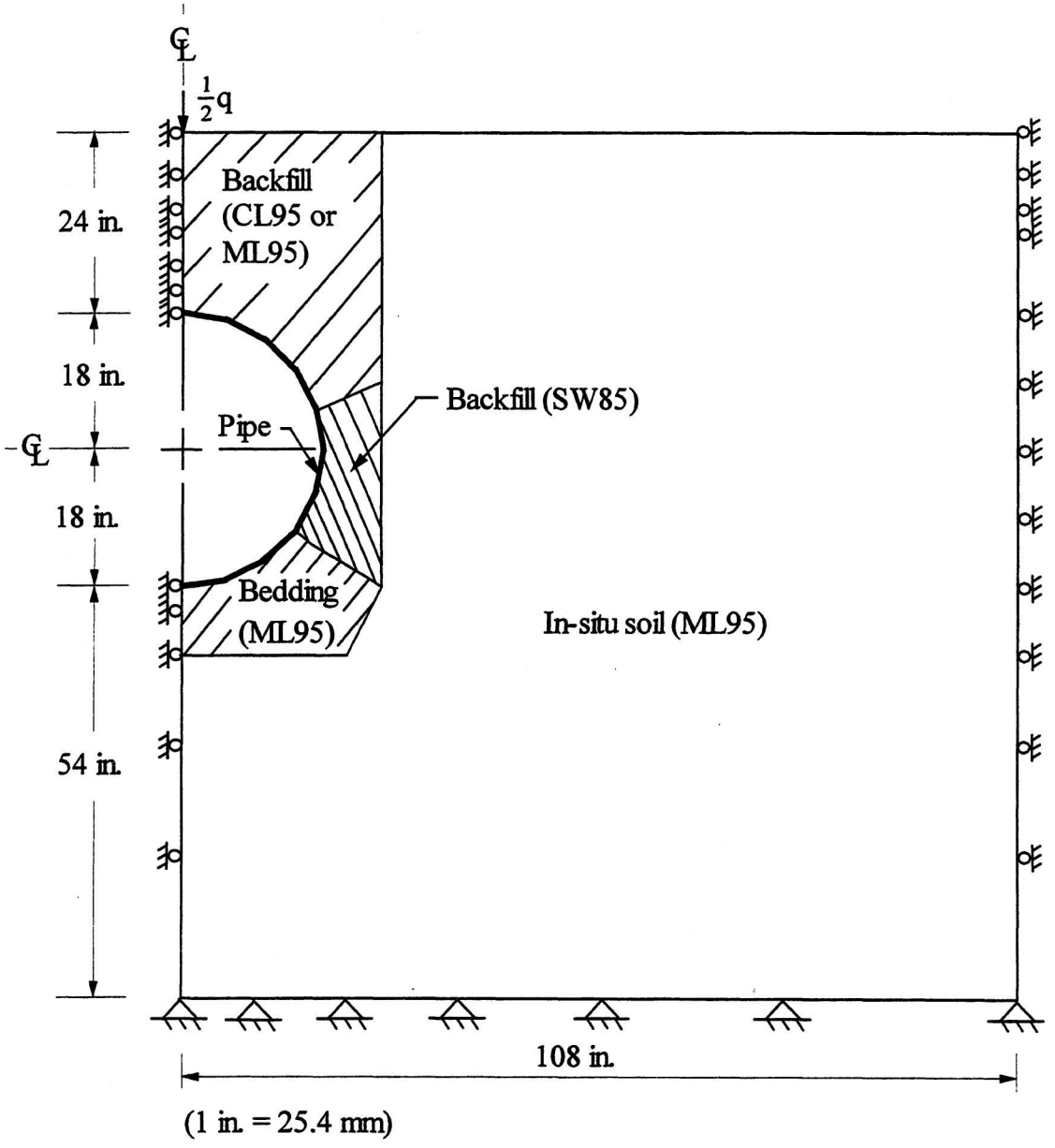

Figure 26. The finite element model of field test ISU9 (mesh shown in Figure 23).

As shown in Figures 27, 28, and 29, the analytical predictions for ISU4, ISU8, and ISU9 do not correspond closely with the field data over the whole range of surface loads. However, both analytical and experimental deflections are less than 1%. The CANDE solutions with backfill ML95 over-estimate the field vertical pipe deflections from the beginning of loading to

Table 11. Duncan soil parameters of the surrounding soil of the field test specimen (as per CANDE).

Soil Name	Soil Type	AASHTO T-99, %	ϕ_o (deg)	$\Delta\phi$ (deg)	C, psi (kPa)	K	n	R_f	K_b	m
SW85	SW	85	38	2	0	450	0.35	0.80	130	0.10
SW90	SW	90	42	4	0	640	0.43	0.75	190[a]	0.05[a]
ML95	ML	95	34	0	4 (28)	440	0.40	0.95	185	0.00
CL95	CL	95	15	4	9 (62)	120	0.45	1.00	80	0.20

[a] - Interpolated value

approximately of 8,000 psf (385 kPa). Beyond this contact stress, the CANDE solutions under-estimate the field data. However, the analytical data with backfill CL95 over-estimate the field data and give relatively conservative predictions. The reasons for these observations are discussed in the following paragraphs.

As described by Ng *(1997)*, the large experimental vertical deflections and the rapid increase in the experimental vertical deflections were likely caused by the load plate punching into the soil cover and the localized bending of the crown of the pipe beneath the load plate. These two phenomena are shown in the photographs Figures 3 and 4, respectively.

The small displacement theory, which is one of the more significant deficiencies of CANDE, limits the capability of CANDE to simulate the localized pipe bending and the punching of the load plate that cause large pipe deflections. This limitation leads to an under-estimation of the pipe deflection for a surface load greater than approximately 8,000 lb (35 kN).

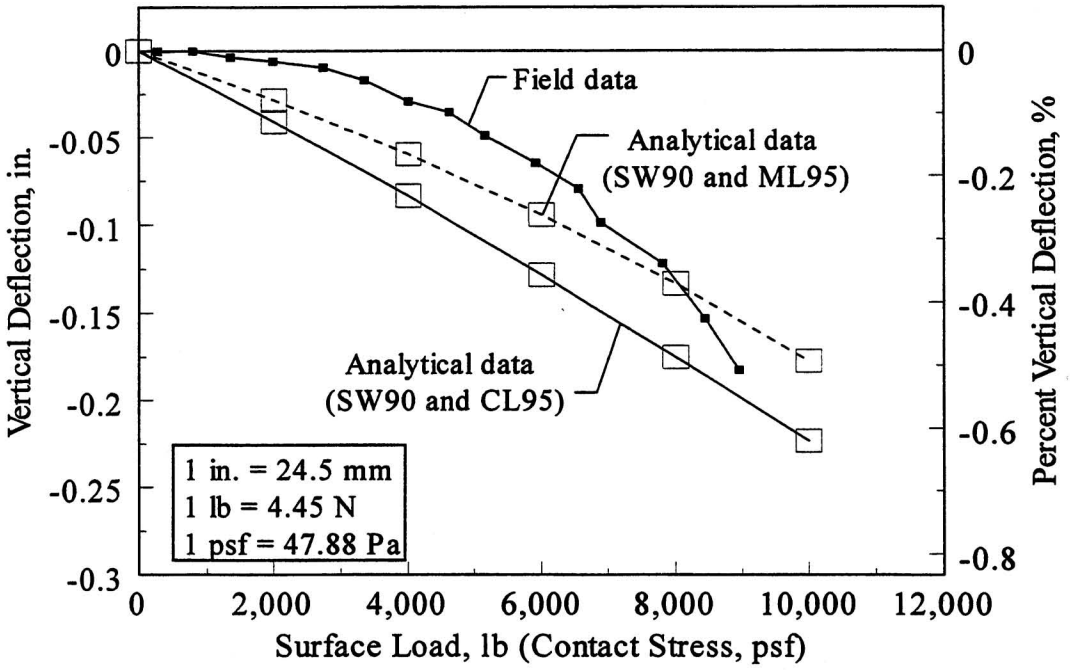

Figure 27. Comparison of ISU4 experimental data with analytical data.

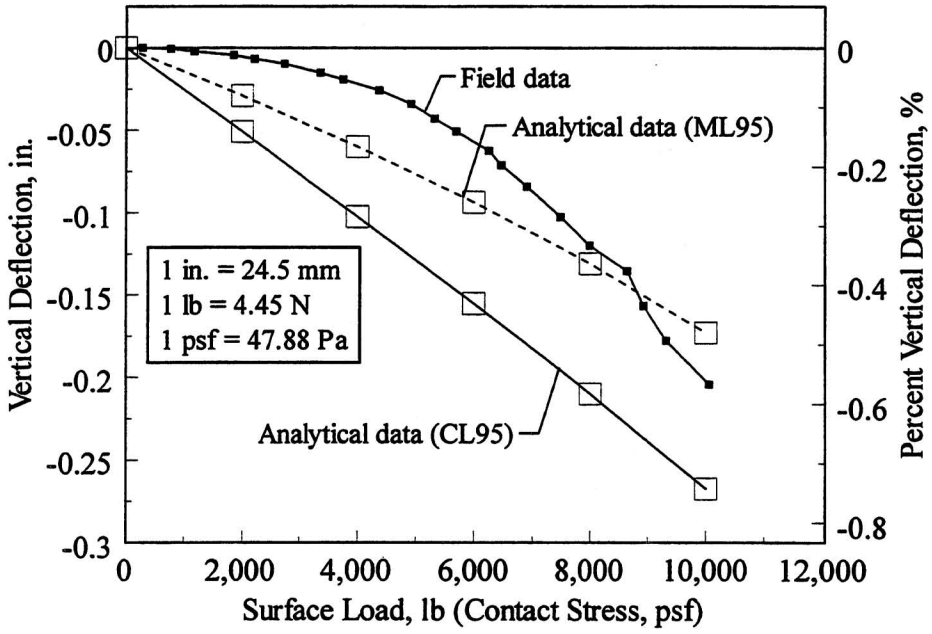

Figure 28. Comparison of ISU8 experimental data with analytical data.

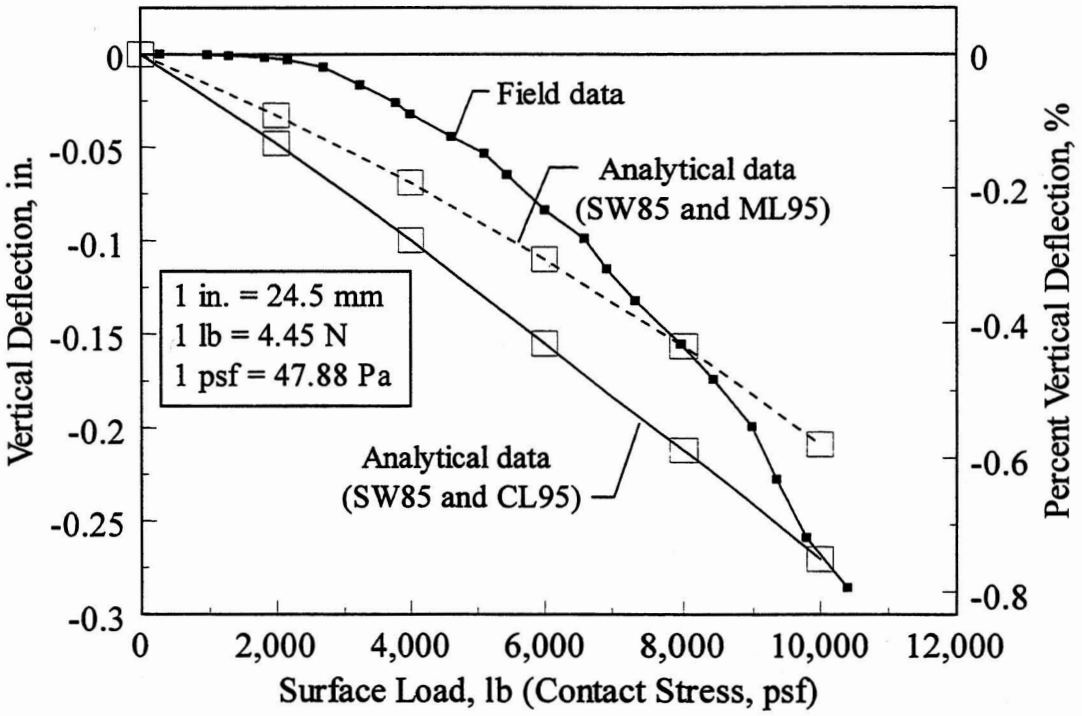

Figure 29. Comparison of ISU9 experimental data with analytical data.

The approximate analytical method that simulates the three dimensional effect of surface loading into a two dimensional response greatly simplifies the actual behavior. The two dimensional system does not account for the longitudinal bending and the changes in longitudinal pipe properties (i.e., effect of corrugation). These limitations will tend to over-estimate pipe vertical deflections as shown in Figures 27 through 29 at a surface load smaller than approximately 8,000 lb (35 kN).

The Duncan soil parameters (Table 11) selected from the CANDE data library do not completely represent the actual soil condition in the field. The difference between the actual stress-strain response of the surrounding soil and the CANDE soil data obviously contributes to the differences between the analytical and experimental data.

4.5. Mesh Sensitivity Under Surface Loads

To illustrate the sensitivity of the finite element mesh used under the surface load, the

analytical and the field data of ISU8 shown in Figure 28 using the mesh shown in Figure 23 were selected as a reference for comparison. The mesh under the surface load is considered because it is the location where the surface load is transmitted to the crown of the pipe and causes the pipe to deflect. The finite element model used for the mesh shown in Figure 23 was modified to generate the new mesh shown in Figure 30 (i.e., the only difference in the CANDE input file is the mesh pattern). Figure 30 illustrates the finer mesh between the location of the surface load and the crown of the pipe. For comparison, soil type ML95 was chosen for both finite element models; the Duncan soil parameters have been presented in Table 11. Pipe vertical deflections obtained from the two finite element models using CANDE are shown in Figure 31 where the modified finite element model predicts a smaller vertical deflection. Comparing with the field data, the modified model and the original model both under-estimate the vertical deflection at surface loads greater than approximately 6,000 lb (27 kN) and 8,000 lb (35 kN), respectively. This demonstration shows that the solutions obtained using CANDE are sensitive to the finite element mesh used under the surface load.

4.6. Analytical Minimum Soil Cover

Katona *(1990)* stated that a minimum of 12 in. (305 mm) of soil cover for plastic pipes suggested by the AASHTO Flexible Culvert Committee is taken directly from the American Iron and Steel Institute (AISI) *(1983)* for corrugated metal culverts. He noted that this requirement is based on the long-time observations by the corrugated steel pipe industry of structural performance under live loads. To provide a better design guideline for plastic pipe designers, finite element models with a mesh similar to Figure 23 were developed using CANDE to determine the minimum soil covers for both 36 in. (915 mm) and 48 in. (1,220 mm) HDPE pipes

from Manufacturers A and C under six different backfill conditions. To simplify computations, only the upper bound of the typical AASHTO H-truck's tire pressure of 100 psi (690 kPa) was used. Furthermore, a conservative tire contact area of 1 ft^2 (0.09 m^2) that gives a concentrated load of 14,400 lb (64 kN) was assumed. A total of twenty four CANDE models were developed for each pipe type: six different backfill conditions and four soil cover heights: 12 in. (305 mm), 24 in. (610 mm), 36 in. (915 mm), and 48 in. (1220 mm). Each CANDE model was based on the previously mentioned approximate analytical method suggested by Katona *(1976)* and the CANDE fundamental analysis assumptions. The manufacturer's pipe properties for the 36 in. (915 mm) and 48 in. (1220 mm) HDPE pipes are shown in Table 10. The Duncan soil model was used to represent the stress-strain responses of the six backfill conditions which are SC85, SC100, SW80, SW95, CL45, and CL95. The bedding and the in-situ soils used in this analysis are ML95 (see Table 11). A lower and a upper bound of the soil compaction were selected for each soil type to represent the "poor" and the "good" backfill conditions, respectively. The Duncan soil parameters of SC85 and SC100, and CL95 have been presented in Tables 9 and 11, respectively. Whereas, the Duncan soil parameters of SW80, SW95, and CL45 are presented in Table 12.

Table 12. Duncan soil parameters of SW80, SW95, and CL45.

Soil Name	Soil Type	AASHTO T-99, %	ϕ_o (deg)	$\Delta\phi$ (deg)	C (psi)	K	n	R_f	K_b	m
SW80	SW	80	36	1	0	320	0.35	0.83	110[a]	0.25[a]
SW95	SW	95	48	8	0	950	0.60	0.70	250	0.0
CL45	CL	45	23	11	0	16	0.95	0.75	15	1.02

[a] - Interpolated value

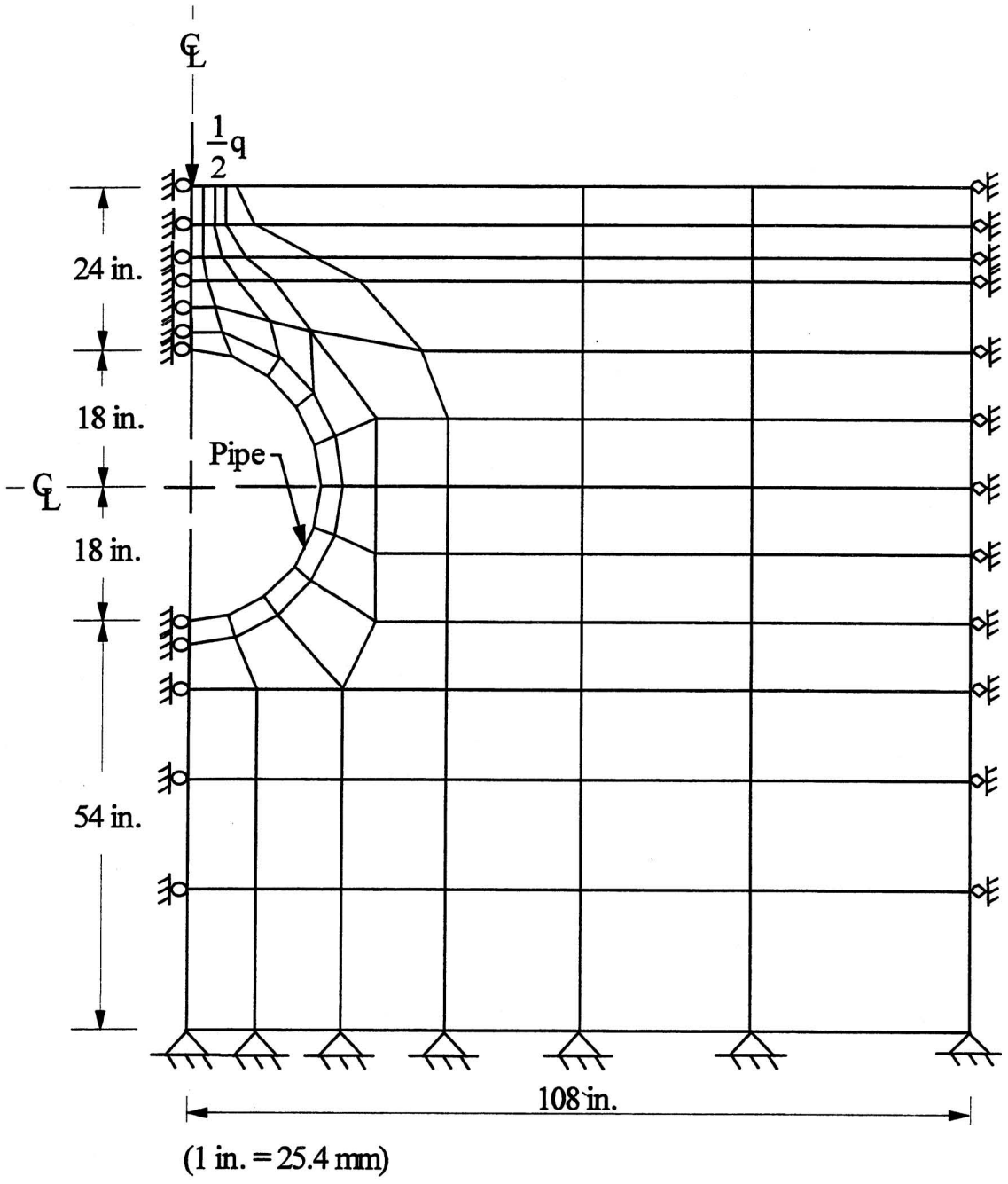

Figure 30. Schematic diagram of the modified finite element mesh of the 36 in. pipe.

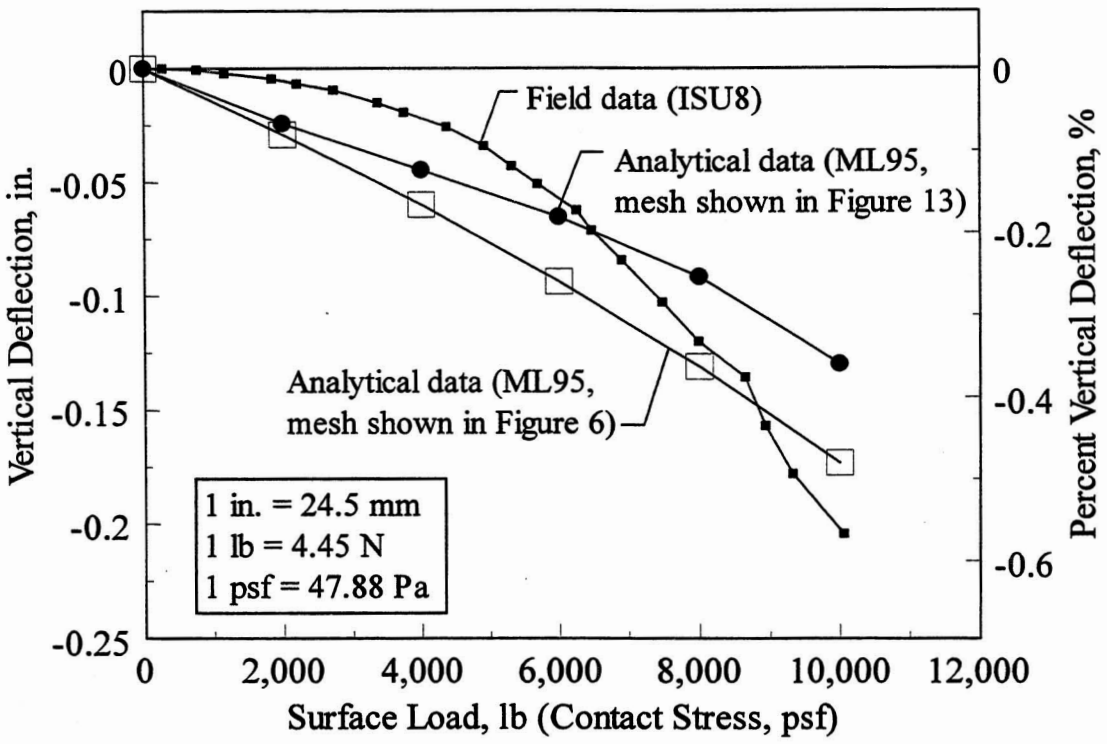

Figure 31. Comparison of the analytical data of the CANDE models for meshes shown in Figures 23 and 30.

Figures 32 through 35 show the CANDE vertical deflection predictions for the four HDPE pipes with six backfill conditions as a function of the soil cover height. The analytical vertical deflection is the total vertical pipe deflection due to the soil cover load and the live load. As shown, the analytical deflections reduce dramatically when the soil cover is increased from 12 in. (305 mm) to 24 in. (610 mm). However, the rate of deflection reduction decreases when the soil cover height is greater than 24 in. (610 mm). Furthermore, both 36 in. (915 mm) and 48 in. (1220 mm) HDPE pipes with a soil cover height of 24 in. (610 mm) or higher and under any of the six backfill conditions meet the 5% deflection criterion. However, this 5% deflection criterion will not be satisfied for these pipes with a 12 in. (305 mm) soil cover and a CL45 backfill. The good backfill condition, CL95, predicts smaller deflection than the poor backfill condition, CL45, and these observations are noted for every type of pipe.

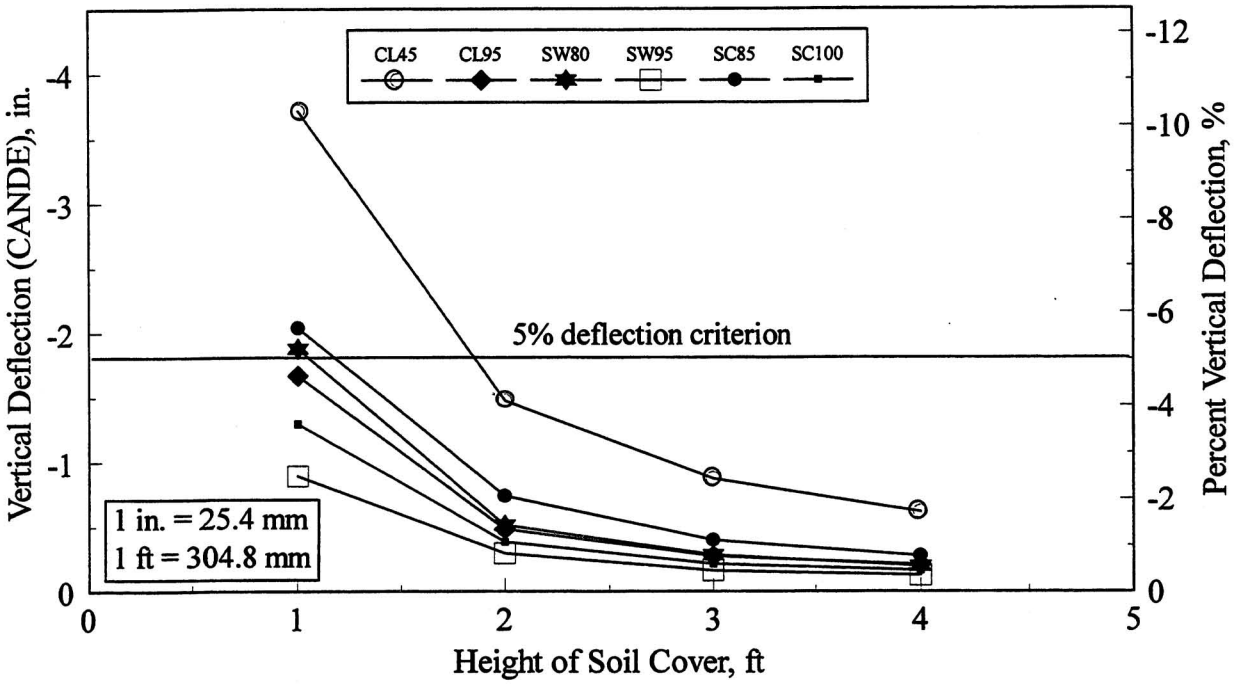

Figure 32. CANDE vertical deflection predictions for 36 in. pipe from Manufacturer A.

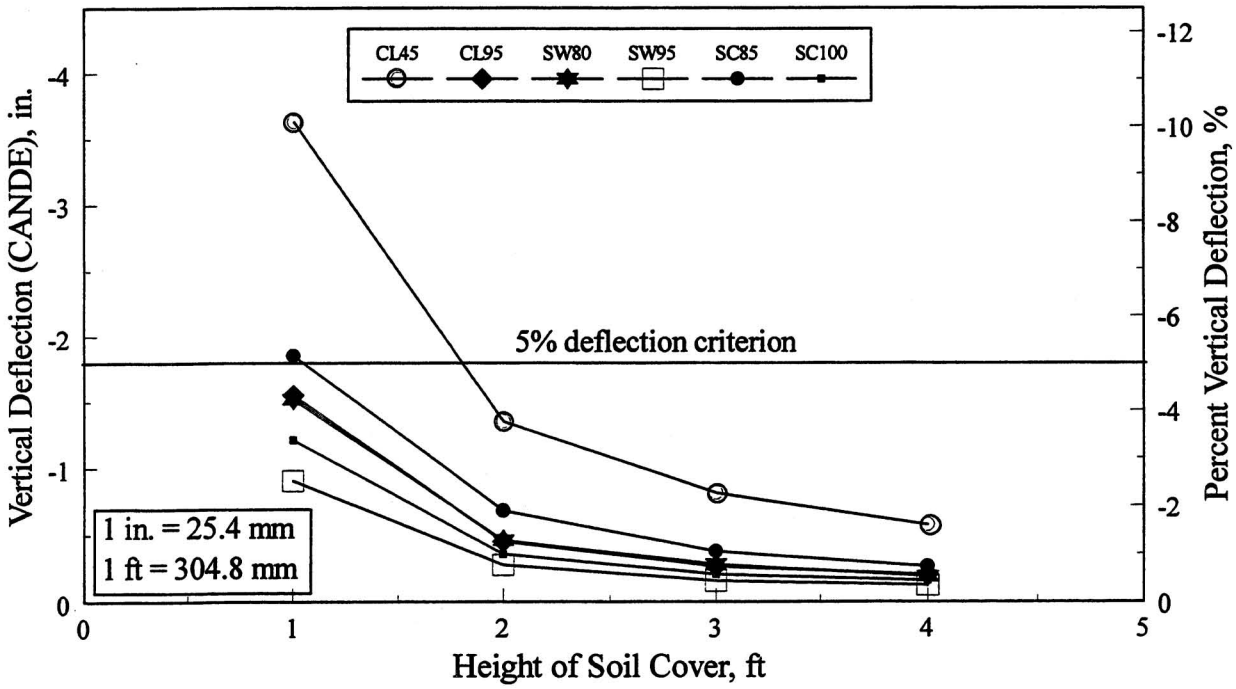

Figure 33. CANDE vertical deflection predictions for 36 in. pipe from Manufacturer C.

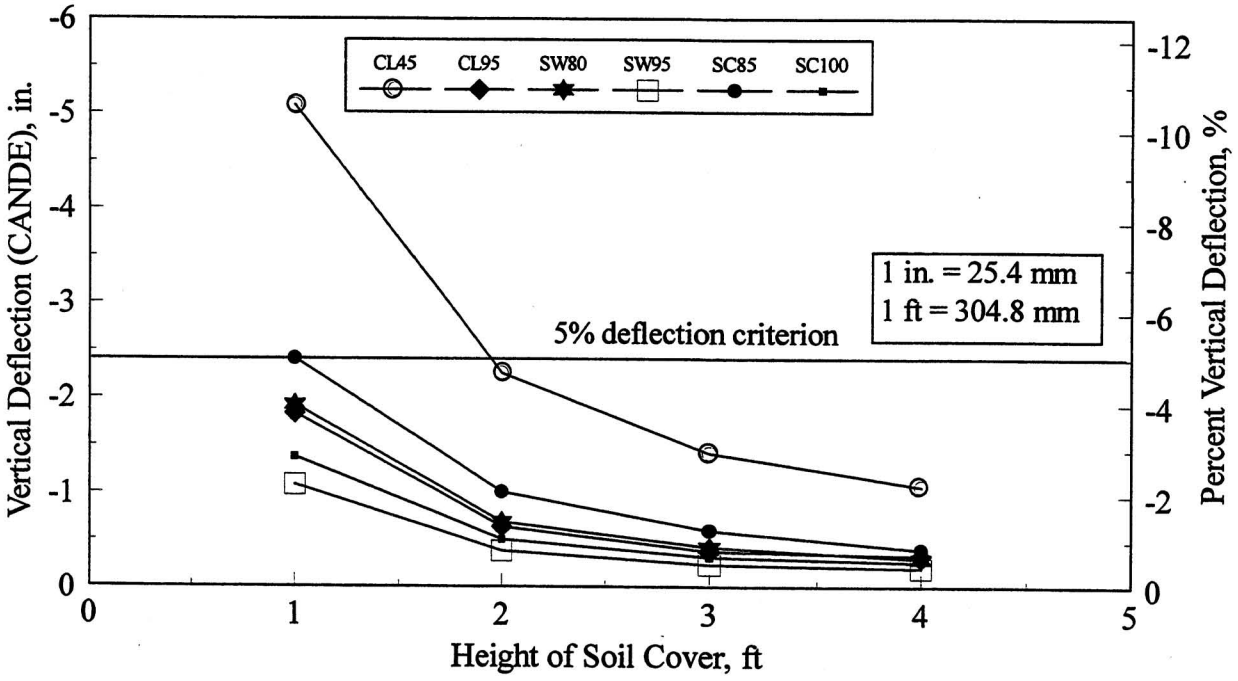

Figure 34. CANDE vertical deflection predictions for 48 in. pipe from Manufacturer A.

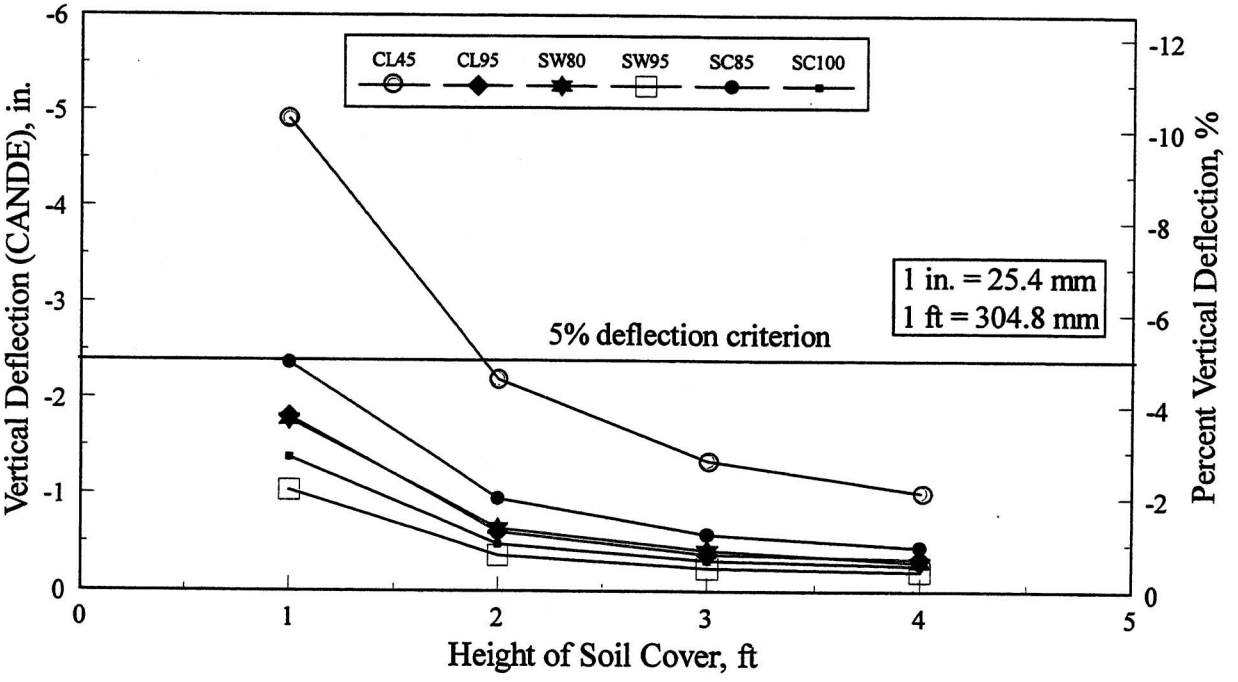

Figure 35. CANDE vertical deflection predictions for 48 in. pipe from Manufacturer C.

Table 13 summarizes the analytical minimum soil cover requirements for the four pipes as a function of type of backfill. The minimum soil cover heights are determined from Figures 32 through 35 where the analytical vertical deflections do not exceed the 5% deflection criterion. In fact, the four design criteria: pipe deflection, outer fiber stress, buckling pressure, and handling performance of the plastic pipe model which were mentioned earlier are considered in this analysis. However, the deflection criterion controls the design for minimum soil cover in all cases. Note that for practical purposes, the minimum soil cover heights presented are 12 in. (305 mm) increments. As mentioned earlier, an absolute minimum requirement of 12 in. (305 mm) soil cover is recommended by the AASHTO Flexible Culvert Committee; however, this requirement is given to maintain the long term serviceability of the HDPE pipes. As shown in Table 13, pipes with the poor backfill condition (CL45) require a minimum soil cover height of 24 in. (610 mm). However, with the good quality backfill (CL95, SW95, and SC100), these pipes only need a minimum of 12 in. (305 mm) soil cover to satisfy all the design criteria. For the SW80 backfill condition, the A36 HDPE pipe with the lowest moment of inertia requires a minimum of 24 in. (610 mm) soil cover. Whereas, the remaining pipes with a relatively larger moments of inertia only need a minimum soil cover of 12 in. (305 mm). Moreover, for the SC85 backfill condition, only the C48 HDPE pipe with the largest moment of inertia needs a 12 in. (305 mm) minimum soil cover, and the remaining pipes require a minimum soil cover of 24 in. (610 mm).

Table 13. Minimum soil cover height in inches.

Pipe	Moment of Inertia, in.^{4}/in. (mm^4/mm)	Backfill Condition					
		CL45	SC85	SW80	SW95	CL95	SC100
A36	0.506 (8,290)	24	24	24	12	12	12
C36	0.55 (9,015)	24	24	12	12	12	12
A48	0.692 (11,340)	24	24	12	12	12	12
C48	0.74 (12,126)	24	12	12	12	12	12

Note: 12 in. = 305 mm, 24 in. = 610 mm.

5. CONCLUSIONS

The test procedures used to evaluate high density polyethylene pipes with a variety of soil backfill is conservative especially where low density fills are loaded to high contact stresses. The failures observed in these tests are the combined effect of soil bearing capacity at the soil surface and localized wall bending of the pipes. Under a pavement system, it is expected that the pipes' performance would be considerably better. With those caveats, the following conclusions are drawn from this study.

1. For most tests the ovalization of the pipes during backfilling induced strains of greater magnitude than under surface loads, provided the loads did not exceed the bearing capacity of the soil cover. The exceptions were the stiffer pipes backfilled with the lower density soils.
2. Glacial till compacted to 50% and 80% provides insufficient support so that pipe failure would occur at surface contact stresses lower than those induced by highway trucks. On the other hand, sand backfill compacted to more than 110 pcf (17.3 KN/m^3) is satisfactory.
3. At low surface contact stresses, deflections are reduced significantly when backfill density is increased from about 50 pcf (7.9 kN/m^3) to 90 pcf (14.1 kN/m^3). Above that unit weight, little improvement in the soil-pipe system is observed.
4. The rate of increase in ultimate strength of the system increases nearly linearly with increasing backfill density.
5. At surface contact stresses approximately equivalent to moderate highway tire pressures applied near the ends of the pipes, pipe deflections are slightly higher than when loaded at the center.
6. Except for low density glacial till, the deflections near the pipe ends are not excessive and the pipes tested here have adequate stiffness.
7. For contact stresses near the upper limit of truck tire pressures and when loaded near the end, pipes with both sand and till backfills fail.

8. For flowable fill backfill, the ultimate capacity of the pipes is nearly doubled and at the upper limit of highway truck tire pressures, deflections are negligible.
9. Pipe specimens tested at ambient laboratory room surface temperatures satisfied AASHTO minimum pipe stiffness requirements at 5% deflection.
10. Nearly all specimens tested at elevated (approximately 120°F (50°C)) surface temperatures failed to meet these requirements.
11. Parallel plate tests at elevated temperatures produced higher deflections at lower loads than at ambient laboratory conditions, however, the location of the heat source had little effect on deflection response.
12. Heating of any portion of the pipe circumference reduced the load carrying capacity of specimens.
13. Parallel plate tests at elevated (approximately 120°F (50°C)) temperatures also produced higher circumferential pipe wall strains for a given load than at ambient temperatures.

6. RECOMMENDED RESEARCH

Based on the literature reviewed, test results, and CANDE Analysis of Phase I (HR-373) and Phase II (HR-373A), the following research is proposed:

1. Similar to CMP installations, there is a potential for uplift failures with PE pipe. An investigation (field testing plus an analytical study) of uplift failures of PE pipe installation should be undertaken. This investigation would include identifying situations in which there are potential for such failures and the development of system(s) to prevent uplift failures.
2. To date, testing has been limited to laboratory and field tests on PE pipes 24 in., 30 in., 36 in., and 48in. (610 mm, 760 mm, 915 mm, 1,220 mm) in diameter. If the DOT has plans in the future on using larger diameter PE pipe, they also should be tested (laboratory and field).
3. At least four demonstration projects should be undertaken. Two ft of cover would be used in all four projects. The variables would be pipe diameter (36 in. and 48 in.) and type of road (Gravel (G) or Concrete pavement (CP)). The four demonstration projects would be as follows: 36 in. (915 mm) diameter + G, 36 in. (915 mm) diameter + CP, 48 in. (1,220 mm) diameter + G, and 48 in. (1,220 mm) diameter + CP. The four PE pipes used in the demonstration projects would be instrumented (strain gages and deflection instrumentation) so that data could be obtained during installation and immediately after installation. All sites would be periodically monitored and load tested for a period of three years after installation.
4. Obtain plans of several existing HDPE pipe installations and use this information as base line data. These installations will be periodically monitored (record any changes in elevations, measure vertical and horizontal diameters so that any changes can be detected,

etc.) for several years after their installation. Hopefully it will be possible to locate, installation with pipes of different diameters, from different manufacturers, with different amounts of cover, with different backfill material, etc.

5. Experimental study of 36 and 48 in. (915 and 1,220 mm) diameter HDPE pipes under dynamic loading and shallow cover.
6. Characterization of Iowa soils with Duncan-Chang constitutive model for application to CANDE and other FEM or numerical geotechnical/structural models used by DOT.

7. ACKNOWLEDGMENTS

The study presented herein (HR-373A) was conducted in conjunction with the Engineering Research Institute of Iowa State University. The research was sponsored by the Project Development Division of the Iowa Department of Transportation and the Iowa Highway Research Board.

The authors wish to thank the various Iowa DOT and county engineers who helped with the project and provided their input and encouragement. In particular, we would like to thank Brad C. Barrett from the Iowa Department of Transportation for his technical input and assistance in various aspects of the investigation.

Appreciation is also extended to Advanced Drainage Systems, Inc. and Hancor, Inc., for their donation of the numerous sections of high-density polyethyelene pipe used in the investigation.

Special thanks are accorded to D. T. Davidson and D. L. Wood, laboratory supervisors, for their assistance with the numerous laboratory and field tests and to the numerous civil engineering and construction engineering undergraduate students who assisted in various aspects of the project.

8. REFERENCES

American Iron and Steel Institute, 1983. Handbook of Steel Drainage and Highway Construction Products American Iron and Steel Institute, Washington, D.C., Third Edition.

Conard, Brett, 1997. "Investigation of high density polyethylene pipe for highway applications: Phase II", Unpublished M.S. Thesis, Iowa State University, Ames, Iowa.

Katona, M. G., 1976. CANDE: A modern approach for the structural design and analysis of buried culverts. FHWA, Report FHWA-RD-77-5, U.S. Department of Transportation.

Katona, M. G., 1990. "Minimum cover heights for corrugated plastic pipe under vehicle loading", *Transportation Research Record* 1288, TRB, National Research Council, Washington, D.C. 1990, pp. 127-135.

Klaiber, F. W., Lohnes, R. A., Wipf, T. J., and Phares, B. M., 1996 Jan. Investigation of high-density polyethylene pipe for highway applications: Phase I. Final Report to the Iowa Department of Transportation.

Meyerhoff, G. G., 1963. "Some research on bearing capacity of foundations", *Canadian Geotechnical Journal*, Vol. 1, No. 1, pp. 16-26.

Musser, S. C., 1989. *CANDE-89 User Manual*, Report No. FHWA-RD-89-169, FHWA, U.S. Dept. of Transportation.

Ng, K. W., 1997. Field tests and analyses of high-density polyethylene pipes for highway application. Unpublished M.S. thesis, Iowa State University, Ames, Iowa.

Phares, Brent, 1996. "Investigation of high density polyethylene pipe for highway applications: Phase I", Unpublished M.S. Thesis, Iowa State University, Ames, Iowa.

Watkins, R. K., R. C. Reeve, and J. B. Goddard, 1983. "Effect of heavy loads on buried corrugated polyethylene pipe", *Transportation Research Record 903*, National Research Council, Washington, D.C., pp. 99-108.